UCSC Cosmology & Galaxy Research Group 2017 – Prof. Joel Primack

UCSC Grad Students:

Christoph Lee christoph28@gmail.com 707-338-9543: Galaxy-Halo Connections, LSS, Halo Properties vs. Density, Stripping, SAM, Deep Learning & Galaxies

Viraj Pandya viraj.pandya@ucsc.edu 831-459-5722 (ISB 255): Galaxies and Cosmology

SIP students supervised by Christoph & Joel:

Austin Tuan (Phillips Academy, Andover, MA) austin.tuan99@gmail.com 408-831-8787: How Does Halo Radial Profile depend on stripping, environment, and other halo properties?

Max Untrecht (Woodside HS) max.untrecht@gmail.com: Halo Properties vs. Mass & Web

Undergraduate Astrophysics Students

Radu Dragomir (UCSC) rdragomi@ucsc.edu: Galaxy Properties from SDSS, Abundance Matching Dependence on Environment

Elliot Eckholm (UCSC) eeckholm@ucsc.edu 619-993-2120: 3D Viz of Cosmic Web & Halos

Sean Larkin (UCSC) sflarkin@ucsc.edu 949-439-7775: Deep Learning & Galaxy Simulations

Yifei Luo (Nanjing U, China) luoyifei54301@sina.com: Identifying SDSS PDGs (Disk Galaxies Without Classical Bulges) and Determining Their Mass, Environment, etc.

Tze Goh (Columbia) tpg2107@columbia.edu: Halo & Galaxy Properties in Small Cosmic Walls (Like Milky Way and Andromeda) and Other Cosmic Web Environments

Graham Vanbenthuysen (UCSC) gvanbent@ucsc.edu 916-508-0446: Galaxy Size vs. Local Density

Other Research Group Members

Miguel Aragon-Calvo (UNAM-Ensenada) miguel.angel.aragon.calvo@gmail.com: Spine of the Cosmic Web of Bolshoi-Planck simulation and SDSS

Peter Behroozi (UC Berkeley) pbehroozi@gmail.com: Galaxies, Galaxy-Halo Connection

Doug Hellinger hellinger.doug@gmail.com: DM Density & V per Voxel, Voids, Protoclusters

Nina McCurdy (Scientific Computing and Imaging Institute, U Utah) nina@cs.utah.edu: Visualizing Forming Galaxies & Dark Matter

Aldo Rodriguez-Puebla (UNAM) rodriguez.puebla@gmail.com: LSS, Galaxies

Paul Sutter (Ohio State) paul@pmsutter.com: Voids in SDSS and in Simulations

Vivian Tang (UCSC) drftingaway@yahoo.com: Shapes of Simulated Galaxies

Dekel Research Group, Hebrew University, Jerusalem

Avishai Dekel (HU) avishai.dekel@mail.huji.ac.il: Galaxy Formation

Santi Roca-Fabrega (HU postdoc) santi.roca@mail.huji.ac.il: galaxy simulations, and streams

Jonathan Freundlich (starting HU postdoc) observations of gas in high-z galaxies, theory

Hangzhou Jiang (starting HU postdoc) working on halos and subhalos

Nir Mandelker (Yale postdoc) nir.mandelker@yale.edu: galaxyVDI, stream instability

UCSC Observational Galaxy Research Group

Guillermo Barro (Berkeley) gbarro@ucolick.org: Galaxy Formation & Evolution, Compaction

Zhu Chen zhuchen@shnu.edu.cn: Galaxy Formation & Evolution

Sandra Faber faber@ucolick.org: Galaxy Formation & Evolution

Yicheng Guo ycguo@ucolick.org: Galaxy Formation & Evolution, Clumps

Marc Huertas-Company (Observatoire de Paris) marc.huertas@obspm.fr: Galaxy Image Analysis with Deep Learning

David Koo koo@ucolick.org: Galaxy Formation & Evolution

Hassen Yesuf hyesuf@ucolick.org: Galaxy Formation & Evolution, Winds

DEEP-Theory Meeting 16 & 23 Jan 2017

TOPICS TODAY

DM halo properties vs. density paper in press; **halo stripping** and **halo radial profile** papers being drafted (with Christoph Lee, Doug Hellinger)

Galaxy R_{eff} = Const (spin parameter)(halo radius) predicts smaller R_{eff} in regions of low environmental density. How to measure R_{eff}?

Constraining the Galaxy Halo Connection: Star Formation Histories, Galaxy Mergers, and Structural Properties, by Aldo Rodriguez-Puebla, Joel, and others (in nearly final form)

Abundance Matching is Independent of Cosmic Environment Density, based on Radu Dragomir's UCSC senior thesis, advised by Aldo and Joel (we're drafting this now)

Analyzing VELA mock images for **clumps** (Yicheng Guo); measuring **GALFIT statistics** a, b, axis ratio b/a, Sersic index of CANDELized images (Yicheng and Vivian Tang) compared with high resolution images (Liz McGrath). **R_{eff} for SDSS galaxies as a function of density** (Christoph, Graham Vanbenthuysen).

Preparing information for deep learning (DL) about the simulations using yt analysis of the saved timesteps (Sean Larkin, Fernando Caro, Christoph Lee) and using other methods (Nir Mandelker, Santi Roca-Fabrega) to see **whether giving the deep learning code this information in addition to mock images will allow the code to determine some of these phenomena from the images** at least in the best cases of inclination, resolution, and signal/noise (Marc Huertas-Company and team). **What data about the simulations should we give DL? Can we make sufficient progress by HST Cycle 24 deadline April 8?**

Galaxy R_{eff} = Const (spin parameter)(halo radius) predicts smaller R_{eff} in regions of low environmental density.

How to measure R_{eff}?

The galaxy data used in the new Somerville+2017 paper to measure r_*,3D came from GAMA Data Release 2, which gave 13,771 galaxies after cuts eliminating Sersic indexes n < 0.3 and n > 10 and eliminating galaxies with sizes r_e < 0.7 arc seconds, according to Section 3.1. Section 3.3 says that the conversion to r_*,3D from r_e,obs = the observed projected effective radius of the light in the same rest-frame waveband is given by

r_e,obs = f_p f_k r_*,3D

where f_p corrects for projection and and f_k is the structural k-correction. The paper quotes f_p = 1 for an edge-on disk, f_p = 0.68 for n = 4, and f_p = 0.61 for n = 1. It summarizes the literature as saying f_k ~ 1.12 to 1.5. The paper says it adopts (f_pf_k)_disk = (1x1.2) = 1.2 and (f_pf_k)_spheroid = (0.68 x 1.15) = 0.78 for spheroids.

Viraj, could you please clarify what rest-frame waveband was used in the Somerville+2017 paper? Presumably the reason you say you need the half-light radius in all 5 SDSS bands u, g, r, i, z is to convert to a fixed rest-frame band, right? Since we are only going out to z ~ 0.15, we may not need to use more than two wavebands. **Viraj**, what source do you suggest we use for the SDSS data we need? (We can also use the GAMA data, but there may not be enough galaxies once we separate into mass and density bins. Still, it would be good to check that we recover the same results in the Somerville+2017 paper using the GAMA data, and bin at least the lower-mass galaxies into a few density bins to see if there is an offset to smaller sizes at lower densities.)

Aldo has suggested using the GIM2D catalog based on SDSS DR7 by Luc Simard+2011 (ApJS 196, 11 with machine-readable tables online at http://vizier.cfa.harvard.edu/viz-bin/VizieR?-source=J/ApJS/196/11 and in http://adsabs.harvard.edu/abs/2011yCat..21960011S). The Simard tables include three different determinations of half-light radii (both a = semimajor axis half-light radius and circularized half-light radius = \sqrt(ab), where b is the minor axis half-light radius), one each for g and r band. Simard also gives the ellipticity e = 1 - b/a for each band. Simard's Table 1 uses n_b = 4 and n_disk free, Table 2 uses both n_bulge and n_disk free, and Table 3 is a single-Sersic fit. **Aldo**, were you suggesting using Table 3, or what? **Viraj**, where should we get the spheroid vs. disk vs. edge-on disk data from?

To get the R_halo for each galaxy, the Somerville+2017 paper uses the Behroozi-Wechsler-Conroy 2013 stellar halo mass relation (SHMR) to assign a stellar mass to every halo in the z = 0.1 halo catalog from the Bolshoi-Planck simulation. (As I emphasized to Rachel, this is inconsistent since BWC13 was based on the Bolshoi simulation with WMAP5/7 cosmological parameters, while Bolshoi-Planck used the rather different Planck parameters which lead to 20-40% more halos at the same Vmax. I thought we had agreed to wait for the updated Planck SHMR which Peter Behroozi promised to send soon, but Rachel instead submitted the paper with this inconsistent use of cosmological parameters; perhaps we can fix this when we respond to the referee. But in our new paper on halo radius vs. environmental density we can consistently use the Planck parameters, using either Peter's new SHMR or the one from the new paper that Aldo is leading.)

Let's discuss this by email and also at the **DEEP-Theory meeting 3-5 pm today (Monday 1/16) in the CfAO Conference Room**.

Joel

On Jan 13, 2017, at 6:42 PM, Viraj Pandya <viraj.pandya@ucsc.edu> wrote:
Hi Joel,
Here is a list of things I'd need from the SDSS database to estimate the 3D half-mass radii of galaxies. The first two are crucial, and the last two might come in handy but aren't 100% necessary right now:

1. half-light radius in u, g, r, i and z bands [necessary]
2. Sersic index in all 5 bands if available, else only in r-band (which SDSS galaxies are selected in) [necessary]
3. axis ratio q:=b/a where b=semi-minor axis and a=semi-major axis [only if easily available]
4. absolute magnitudes in u, g, r, i and z bands [only if easily available]

Viraj

Constraining the Galaxy-Halo Connection Over The Last 13.3 Gyrs: Star Formation Histories, Galaxy Mergers and Structural Properties

Aldo Rodríguez-Puebla[1,2⋆], Joel Primack[3] et al.

[1] *Department of Astronomy & Astrophysics, University of California at Santa Cruz, Santa Cruz, CA 95064, USA*
[2] *Instituto de Astronomía, Universidad Nacional Autónoma de México, A. P. 70-264, 04510, México, D.F., México*
[3] *Physics Department, University of California, Santa Cruz, CA 95064, USA*

ABSTRACT

We present new determinations of the stellar-to-halo mass relation at $z = 0 - 10$ that match the evolution of the galaxy stellar mass function, the SFR $- M_*$ relation, and the cosmic star formation rate. We utilize a large compilation of more than 40 observational studies from the literature and correct them for potential biases that could affect our determinations. Using our robust determinations of the SHMR and the halo mass assembly, we study the star formation histories, merger rates and the structural properties of galaxies. Our findings are: (1) The transition halo mass above/below which galaxies are observed to be statistically star-forming/quenched is when sSFR/sMAR~ 1, where sMAR is the specific halo mass accretion rate. (2) This transition halo mass depends on redshift, at $z \sim 0$ it is $M_{\rm vir} \sim 10^{12}{\rm M}_\odot$ while at $z \sim 3$ it is $M_{\rm vir} \sim 10^{13}{\rm M}_\odot$, presumably due to cold streams being more efficient at high redshift while virial shocks became more relevant at lower redshifts, as theoretically expected. (3) Unexpectedly, the ratio sSFR/sMAR has a peak value, which occurs around $M_{\rm vir} \sim 2\times10^{11}{\rm M}_\odot$. (4) The mass density within 1 kpc, Σ_1, is a good indicator of the global sSFR. (5) galaxies are statistically quenched once they reached a maximum in Σ_1, consistent with theoretical expectations of the gas compaction model. (6) This maximum of Σ_1 depends on redshift. (7) Galaxies grow primarily due to in-situ star formation but massive galaxies could have assembled $\sim 20\%$ of their mass through galaxy mergers. (8) While minor mergers are more frequent, major mergers have contributed $\sim 80\%$ of the accreted stellar mass in massive galaxies but only $\sim 40\%$ in MW sized galaxies. (9) The marked change in the slope of the size–mass relation when galaxies became quenched, from $d\log R_{\rm eff}/d\log M_* \sim 0.35$ to ~ 2.5, could be the result of dry minor mergers.

Constraining the Galaxy Halo Connection: Star Formation Histories, Galaxy Mergers, and Structural Properties, by Aldo Rodriguez-Puebla, Joel, and others (in nearly final form)

PREVIEW

Table 1. Observational data on the galaxy stellar mass function

Author	Redshift[a]	Ω [deg^2]	Corrections
Bell et al. (2003)	$z \sim 0.1$	462	I+SP+C
Yang, Mo & van den Bosch (2009a)	$z \sim 0.1$	4681	I+SP+C
Li & White (2009)	$z \sim 0.1$	6437	I+P+C
Bernardi et al. (2010)	$z \sim 0.1$	4681	I+SP+C
Bernardi et al. (2013)	$z \sim 0.1$	7748	I+SP+C
Rodriguez-Puebla et al. in prep	$z \sim 0.1$	7748	S
Drory et al. (2009)	$0 < z < 1$	1.73	SP+C
Moustakas et al. (2013)	$0 < z < 1$	9	SP+D+C
Pérez-González et al. (2008)	$0.2 < z < 2.5$	0.184	I+SP+D+C
Tomczak et al. (2014)	$0.2 < z < 3$	0.0878	C
Ilbert et al. (2013)	$0.2 < z < 4$	2	C
Muzzin et al. (2013)	$0.2 < z < 4$	1.62	I+C
Santini et al. (2012)	$0.6 < z < 4.5$	0.0319	I+C
Mortlock et al. (2011)	$1 < z < 3.5$	0.0125	I+C
Marchesini et al. (2009)	$1.3 < z < 4$	0.142	I+C
Stark et al. (2009)	$z \sim 6$	0.089	I
Lee et al. (2012)	$3 < z < 7$	0.089	I+SP+C
González et al. (2011)	$4 < z < 7$	0.0778	I+C
Duncan et al. (2014)	$4 < z < 7$	0.0778	C
Song et al. (2015)	$4 < z < 8$	0.0778	I
This paper, Appendix D	$4 < z < 10$	0.0778	–

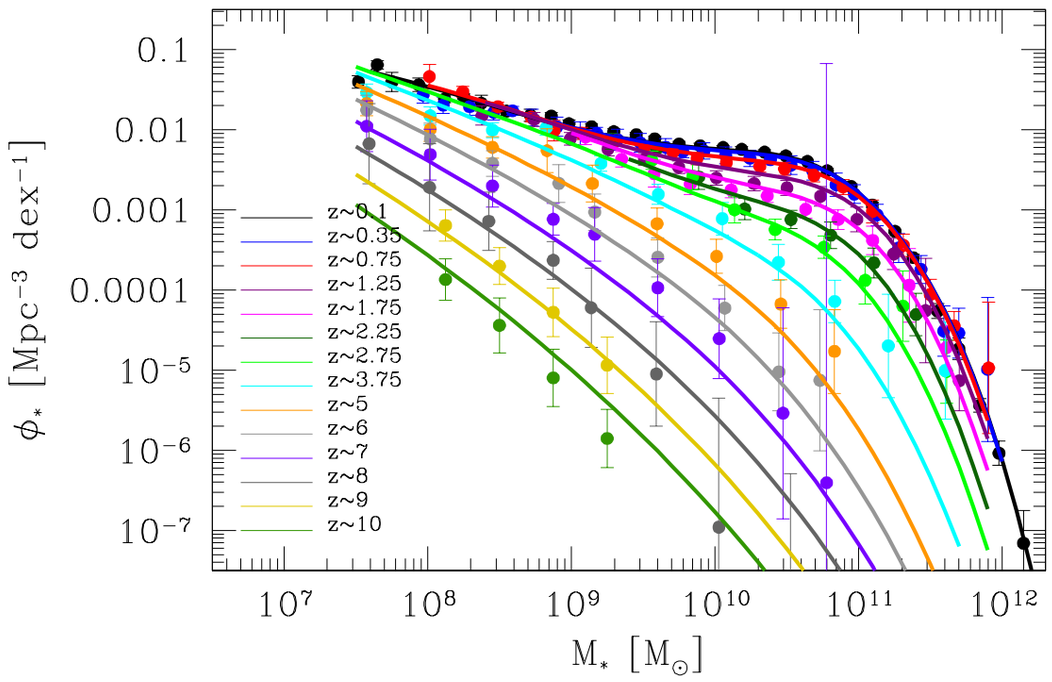

Figure 2. Redshift evolution from $z \sim 0.1$ to $z \sim 10$ of the galaxy stellar mass function (GSMF) derived by using 22 observational samples from the literature and represented with the

Table 2. Observational data on the star formation rates

Author	Redshift[a]	SFR Estimator	Corrections	Type
Chen et al. (2009)	$z \sim 0.1$	H_α/H_β	S	All
Salim et al. (2007)	$z \sim 0.1$	UV SED	S	All
Noeske et al. (2007)	$0.2 < z < 1.1$	UV+IR	S	All
Karim et al. (2011)	$0.2 < z < 3$	1.4 GHz	I+S+E	All
Dunne et al. (2009)	$0.45 < z < 2$	1.4 GHz	I+S+E	All
Kajisawa et al. (2010)	$0.5 < z < 3.5$	UV+IR	I	All
Whitaker et al. (2014)	$0.5 < z < 3$	UV+IR	I+S	All
Sobral et al. (2014)	$z \sim 2.23$	H_α	I+S+SP	SF
Reddy et al. (2012)	$2.3 < z < 3.7$	UV+IR	I+S+SP	SF
Magdis et al. (2010)	$z \sim 3$	FUV	I+S+SP	SF
Lee et al. (2011)	$3.3 < z < 4.3$	FUV	I+SP	SF
Lee et al. (2012)	$3.9 < z < 5$	FUV	I+SP	SF
González et al. (2012)	$4 < z < 6$	UV+IR	I+NE	SF
Salmon et al. (2015)	$4 < z < 6$	UV SED	I+NE+E	SF
Bouwens et al. (2011)	$4 < z < 7.2$	FUV	I+S	SF
Duncan et al. (2014)	$4 < z < 7$	UV SED	I+NE	SF
Shim et al. (2011)	$z \sim 4.4$	H_α	I+S+SP	SF
Steinhardt et al. (2014)	$z \sim 5$	UV SED	I+S	SF
González et al. (2010)	$z = 7.2$	UV+IR	I+NE	SF
This paper, Appendix D	$4 < z < 8$	FUV	I+E+NE	SF

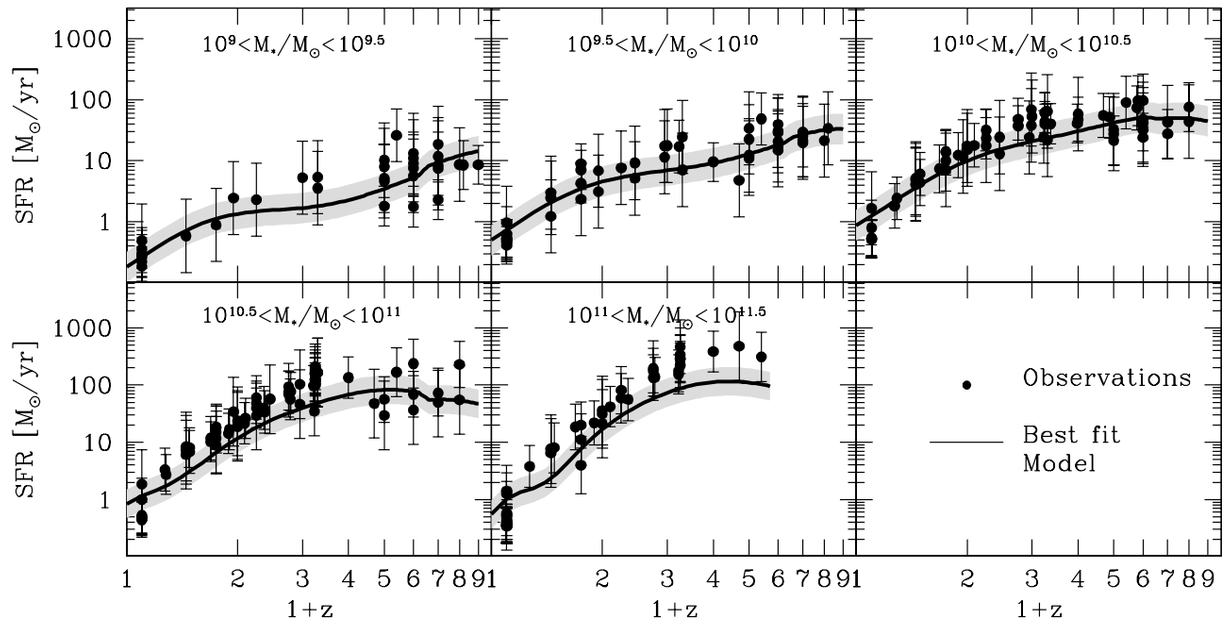

Figure 3. Star formation rates as a function of redshift z in five stellar mass bins. Black solid lines shows the resulting best fit model to the SFRs implied by our model. The filled circles with error bars show the observed data as described in the text, see Section 2.

Constraining the Galaxy Halo Connection: Star Formation Histories, Galaxy Mergers, and Structural Properties, by Aldo Rodriguez-Puebla, Joel, and others (in nearly final form) PREVIEW

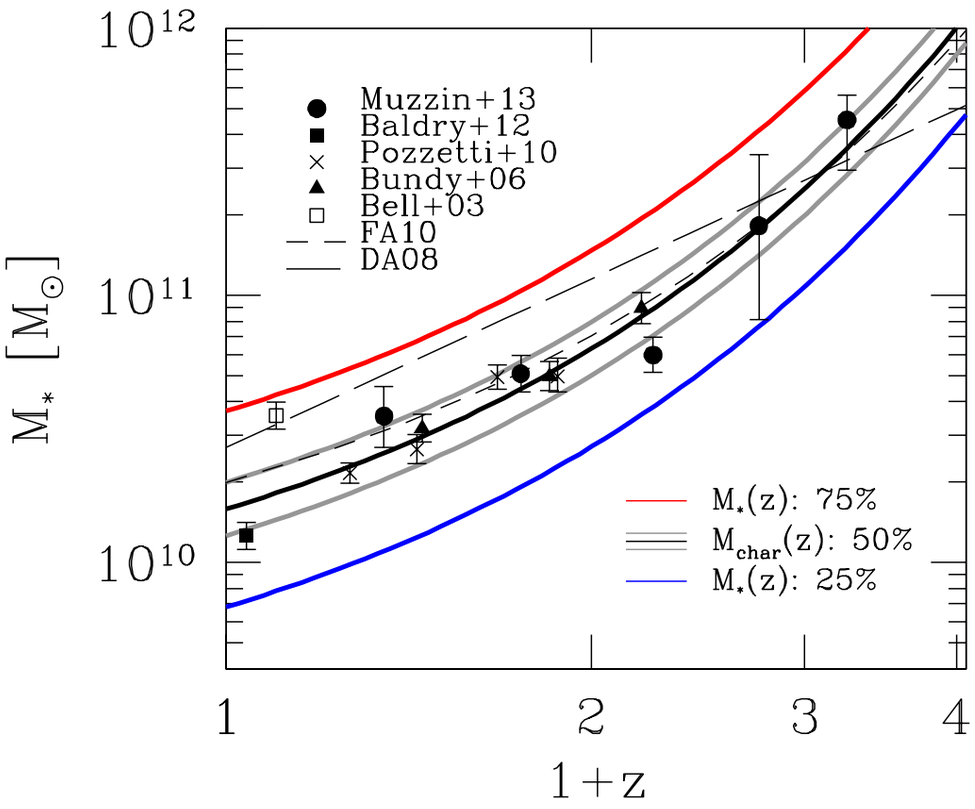

Figure 1. Transition stellar mass $M_{\rm char}(z)$ at which the fractions of blue star forming and red quenched galaxies are both 50%. The open square with error bars shows the transition mass for local galaxies as derived in Bell et al. (2003) based on the SDSS DR2, while the filled triangles show the transition mass derived in Bundy et al. (2006) based on the DEEP2 survey. Drory & Alvarez (2008) based on the FORS Deep Field survey is indicated with the long dashed line; observations from Pozzetti et al. (2010) based on the COSMOS survey are indicated with the skeletal symbols; observations from Baldry et al. (2012) based on the GAMA survey are shown with filled square; and observations from Muzzin et al. (2013) based on the COSMOS survey, are shown as filled circles. The empirical results based on abundance matching by Firmani & Avila-Reese (2010) are shown with the short dashed lines. The solid black line shows the relation $\log(M_{\rm char}(z)/{\rm M}_\odot) = 10.2 + 0.6z$, employed in this paper and that is consistent with most of the above studies. The gray solid lines show the results when shifting $(M_{\rm char}(z)/{\rm M}_\odot)$ 0.1 dex higher and lower. The red (blue) curves show the stellar mass vs. z where 75% (25%) of the galaxies are quenched.

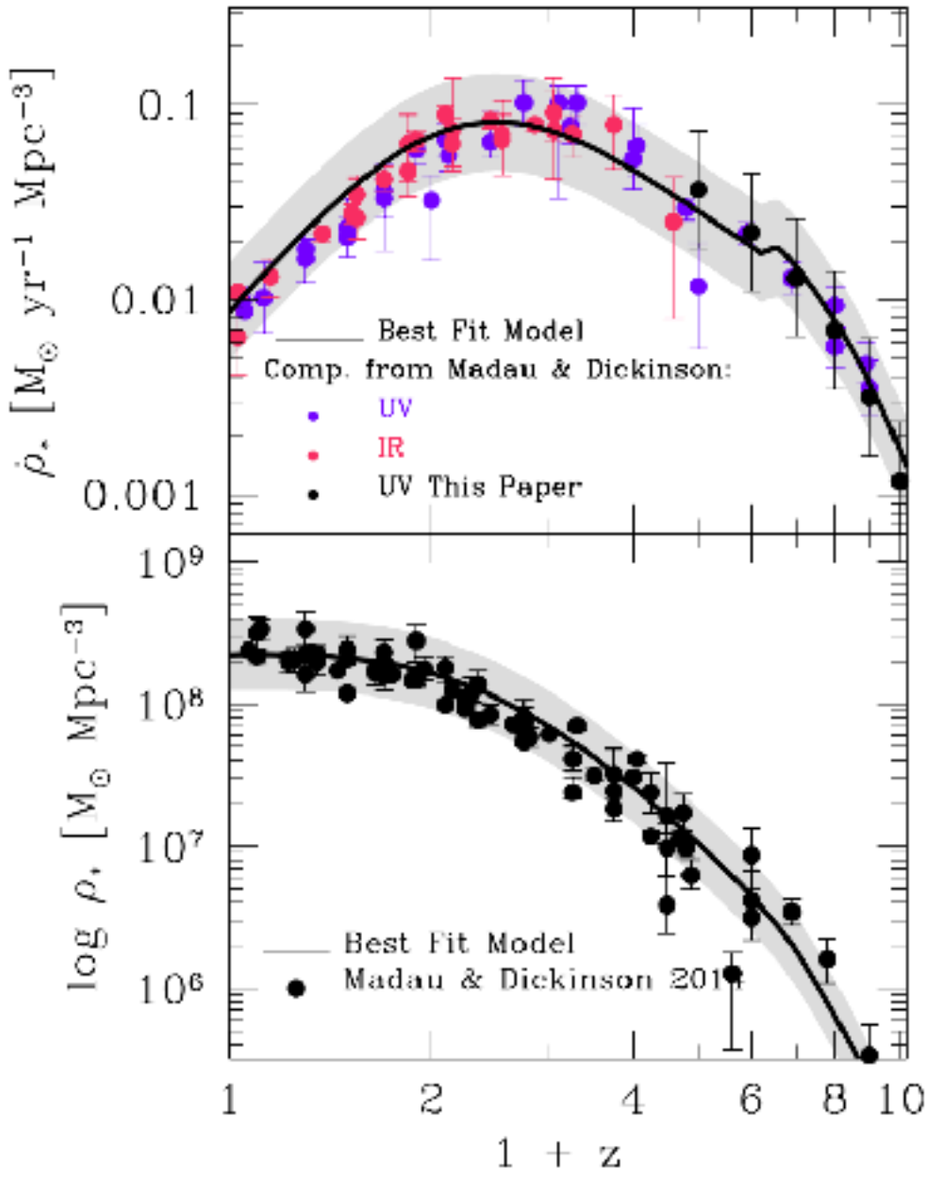

Figure 5. Upper Panel: Cosmic star formation rate, CSFR. The solid black line shows the resulting best fit model to the CSFR as described in Section 2.4. Filled red and violet circles show a set of compiled observations by Madau & Dickinson (2014) from FUV+IR rest frame luminosities. UV luminosities are dust-corrected. Black solid circles show the results from the UV dust-corrected luminosity functions described in Appendix D. **Lower Panel:** Cosmic stellar mass density. The solid black line shows the predictions for our best fit model. Filled black circles show the data points compiled in Madau & Dickinson (2014). All data was adjusted to the IMF of Chabrier (2003). In both panels, the light grey shaded area shows the systematic assumed to be of 0.25 dex.

Constraining the Galaxy Halo Connection: Star Formation Histories, Galaxy Mergers, and Structural Properties, by Aldo Rodriguez-Puebla, Joel, and others (in nearly final form) PREVIEW

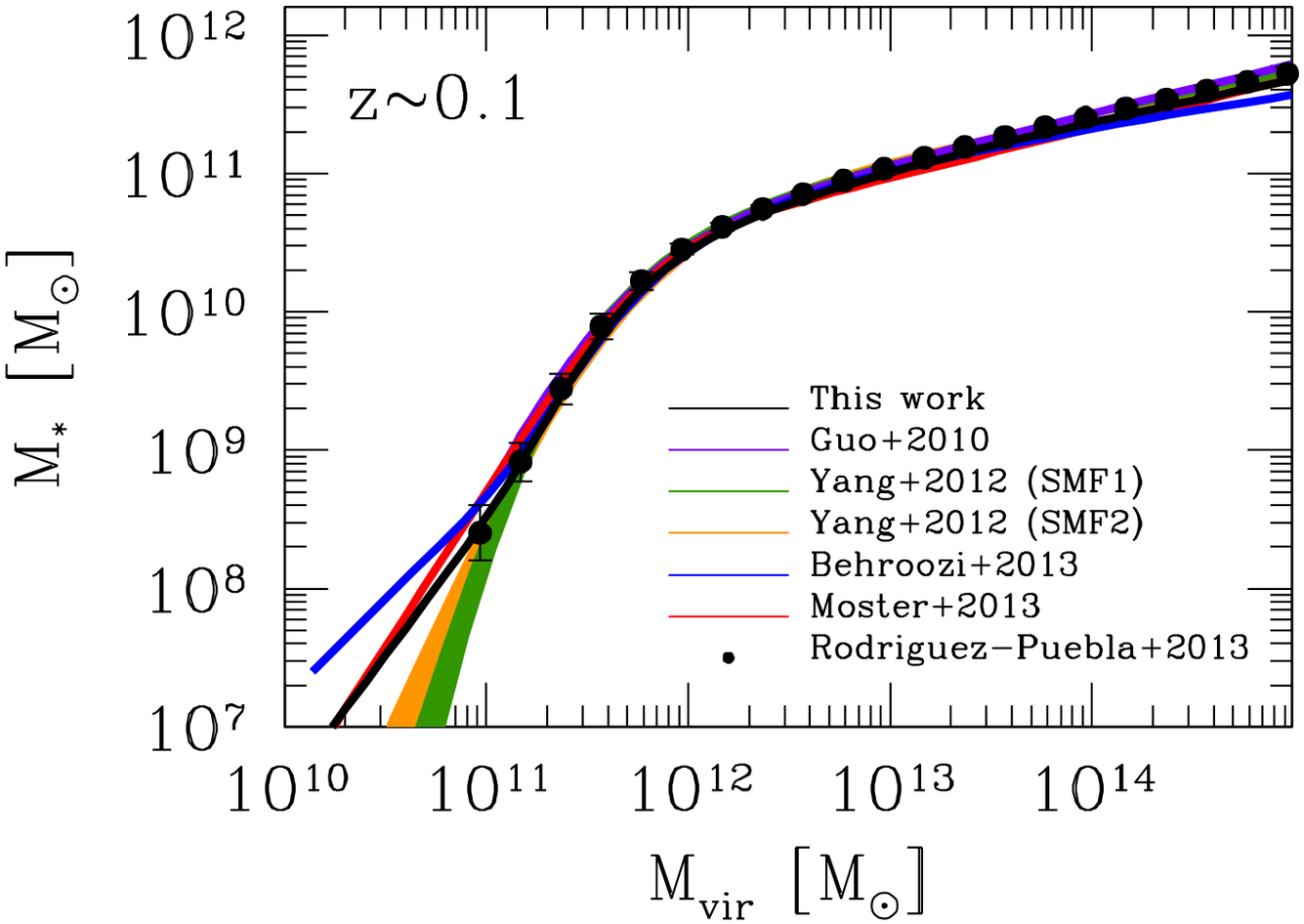

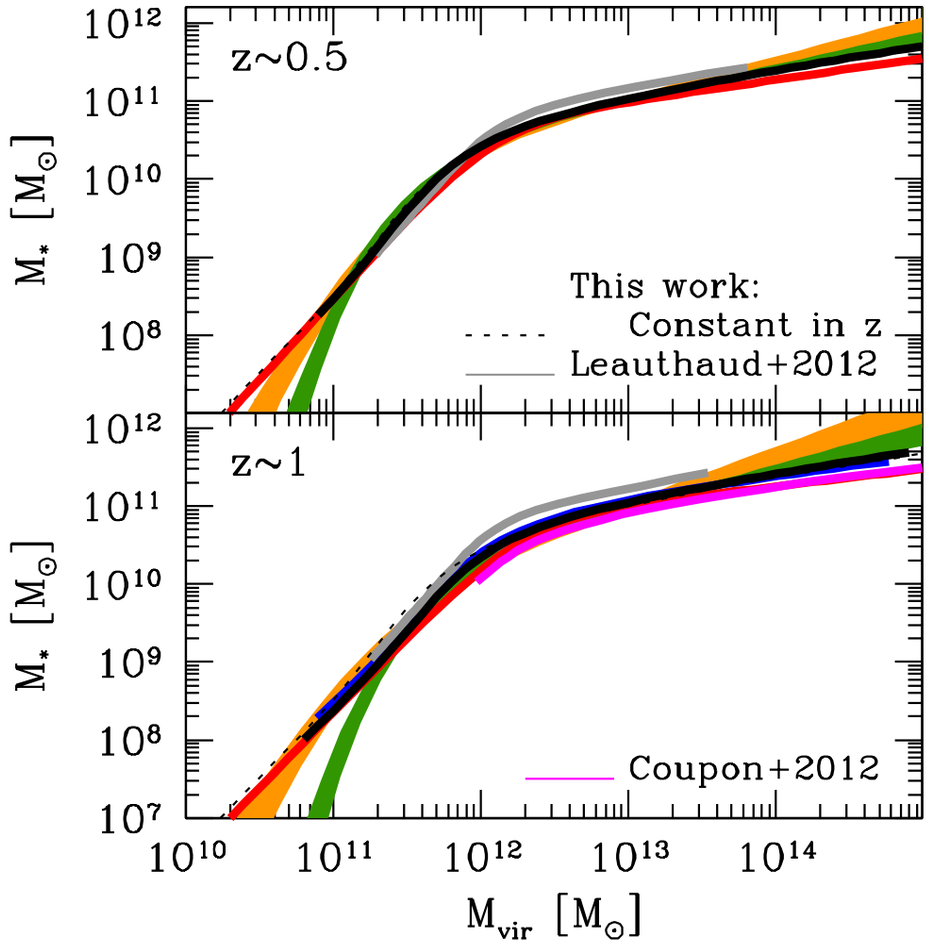

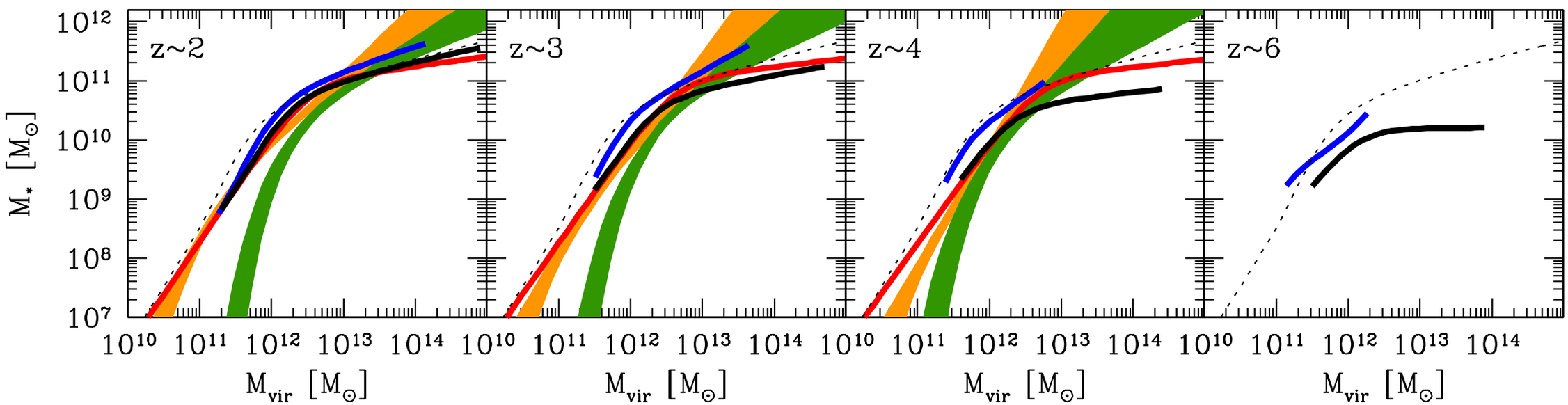

Constraining the Galaxy Halo Connection: Star Formation Histories, Galaxy Mergers, and Structural Properties, by Aldo Rodriguez-Puebla, Joel, and others (in nearly final form) PREVIEW

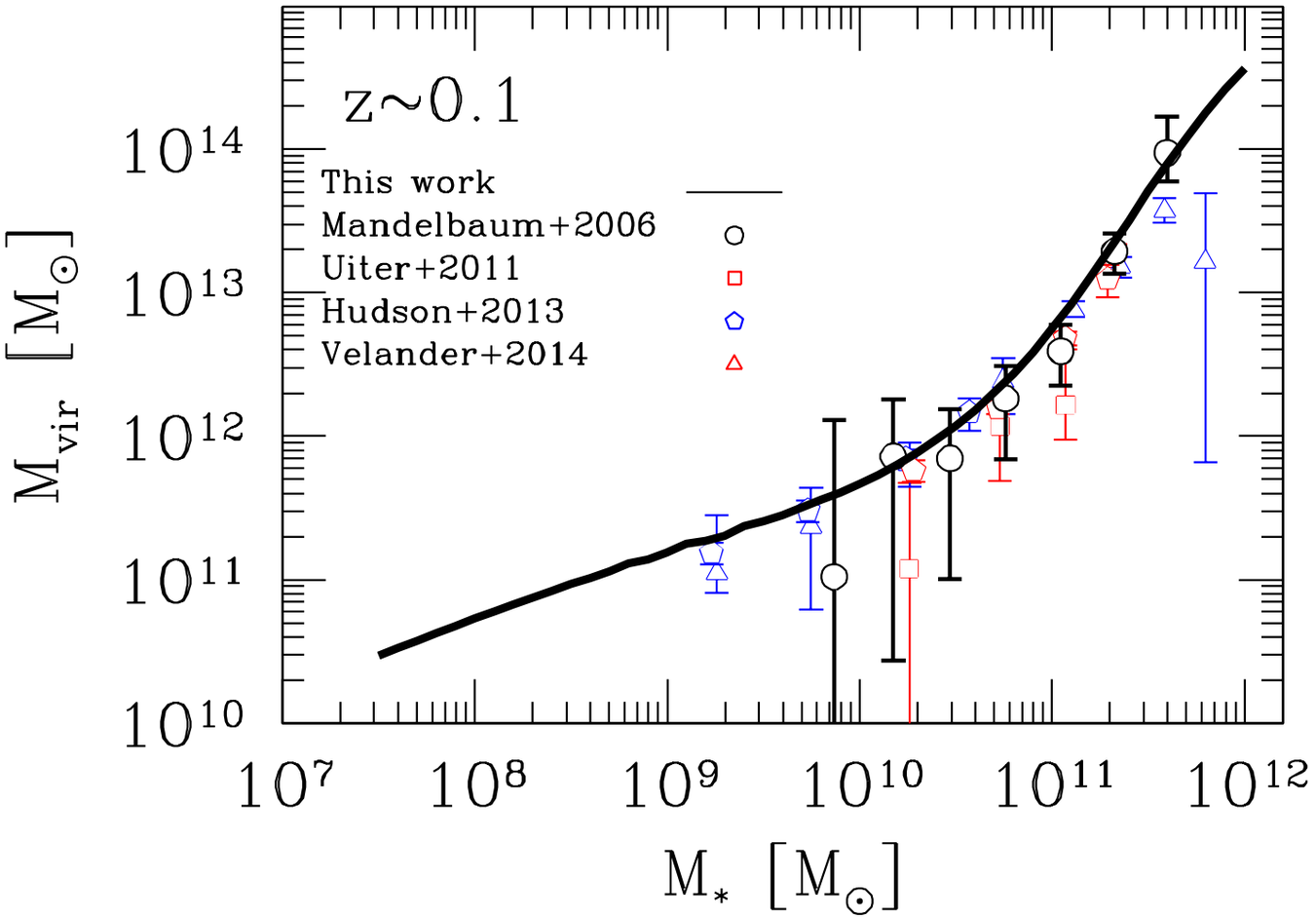

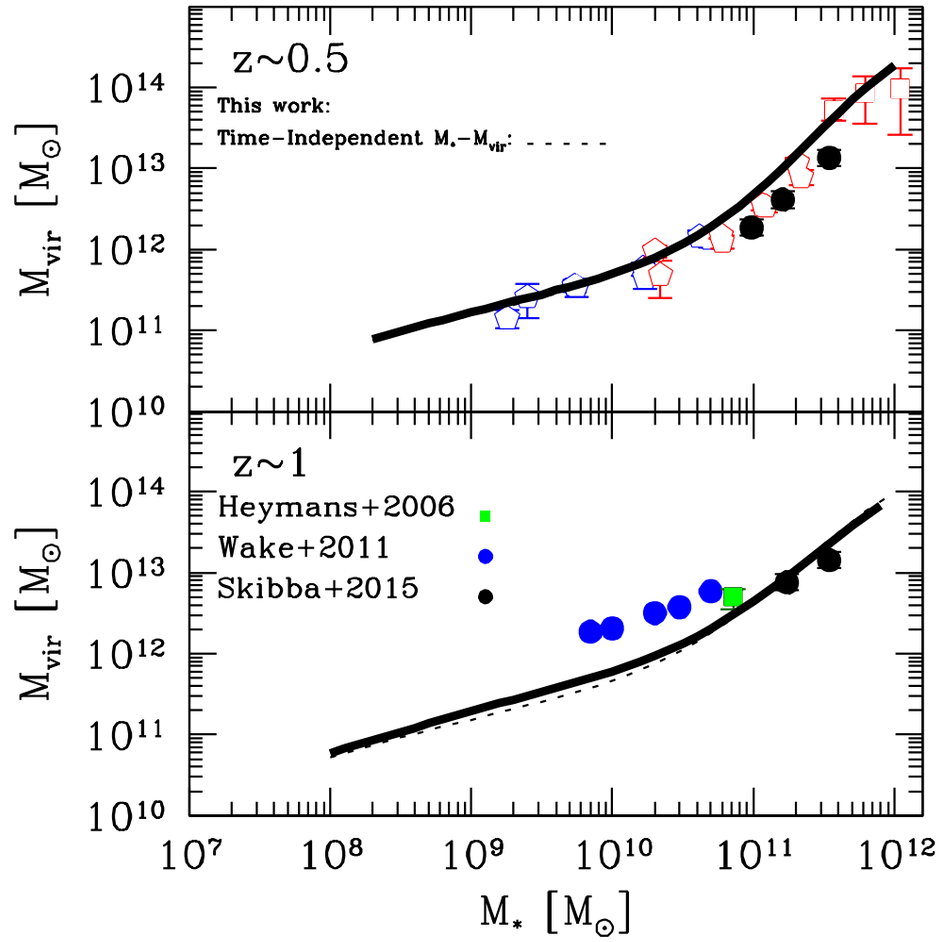

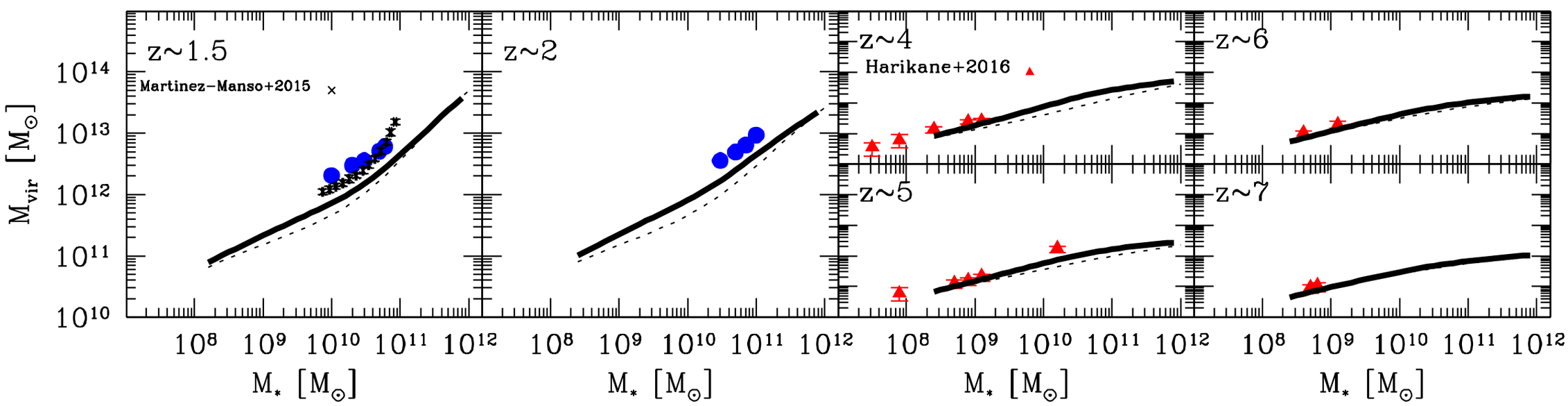

Distributions at a fixed Halo Mass: Assumption in SHAM

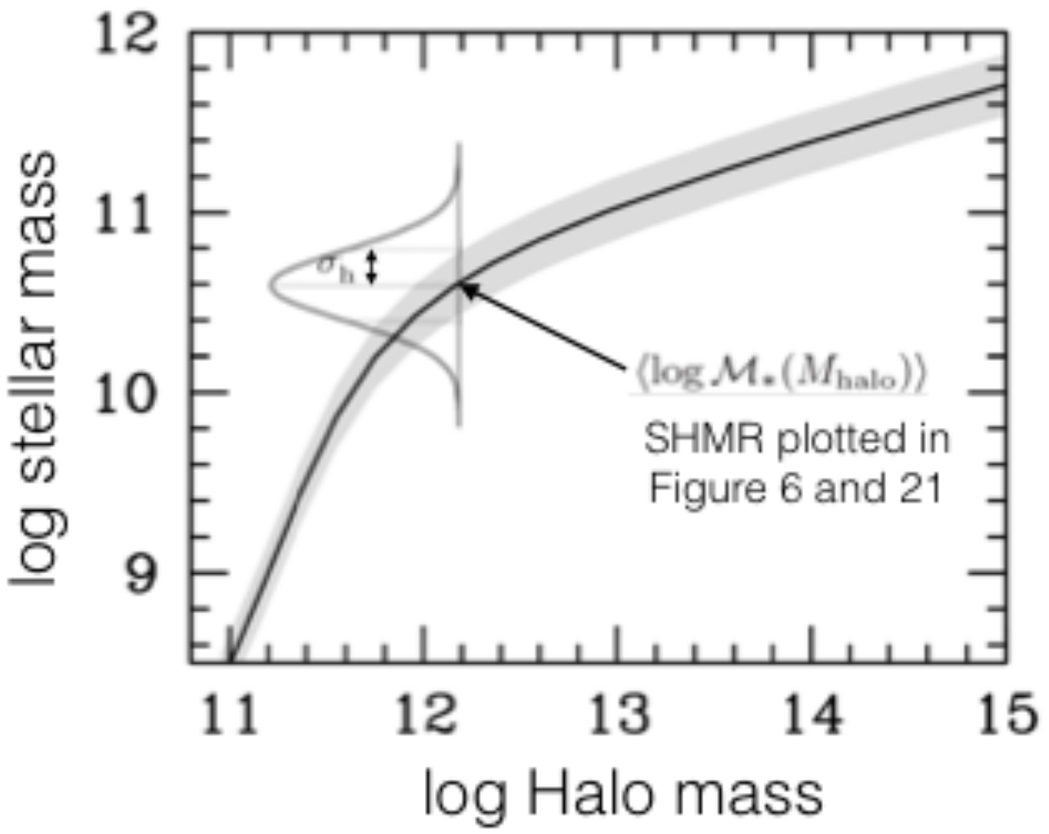

$$\mathcal{H}(M_*|M_{halo}) = \frac{1}{\sqrt{2\pi\sigma_h^2}} \exp\left[-\frac{(\log M_* - \langle \log \mathcal{M}_*(M_{halo})\rangle)^2}{2\sigma_h^2}\right]$$

Galaxies are randomly distributed around the mean relation (solid black line, $\langle \log \mathcal{M}_*(M_{halo}) \rangle$ by following a gaussian distribution with dispersion σ_h

Distributions at a fixed Stellar Mass: Observationa papers that select stellar ma bins/thresholds

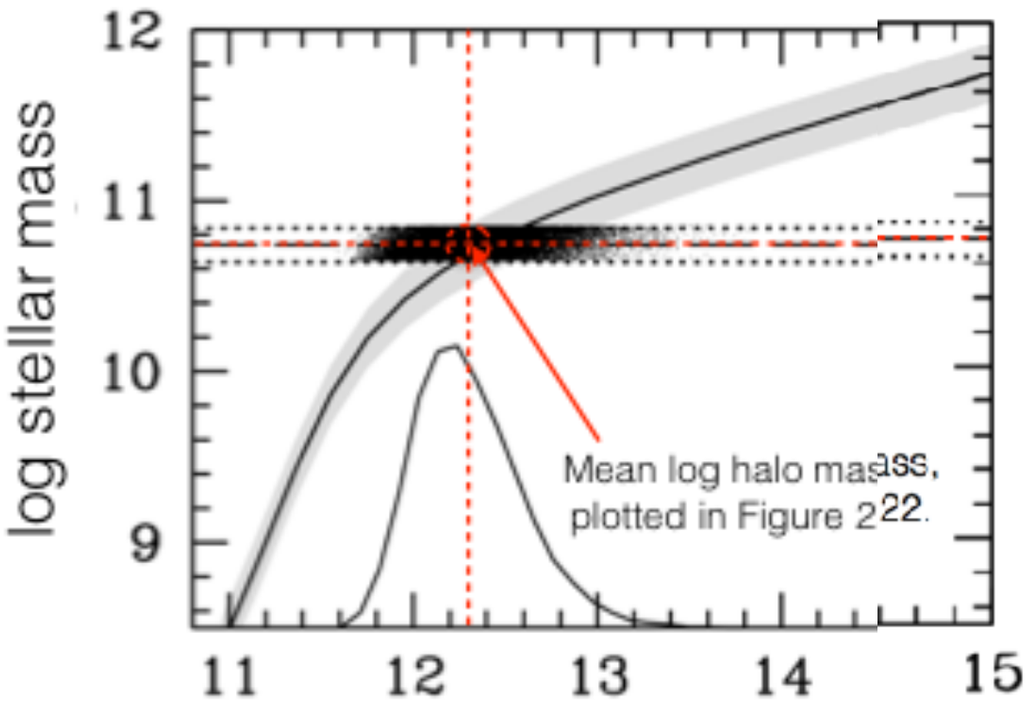

When selecting galaxies at a fixed M*, the points are not longer distributed as Gaussians. The mean log halo mass is not longer located in the solid black line but is slightly shifted towards low halo masses. This is more dramatic at high masses. The reason is that the distribution of points at a fixed stellar mass depends on the number density of galaxies and halos.

SFR DATA & FITS

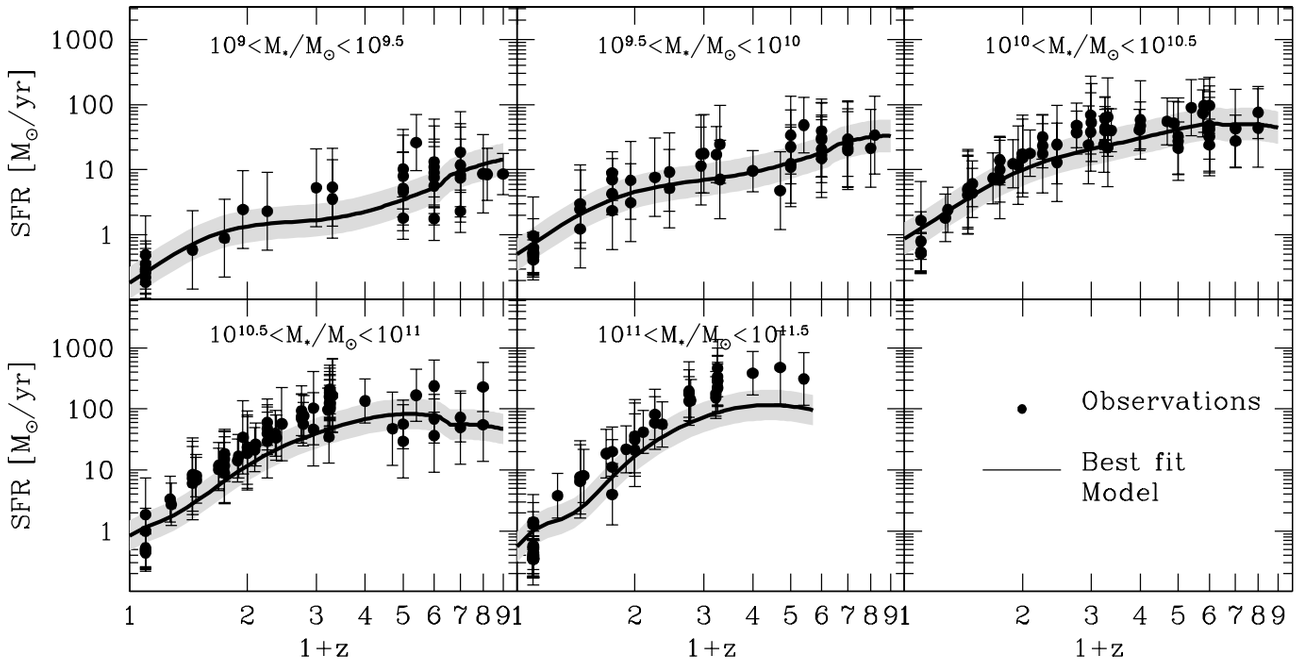

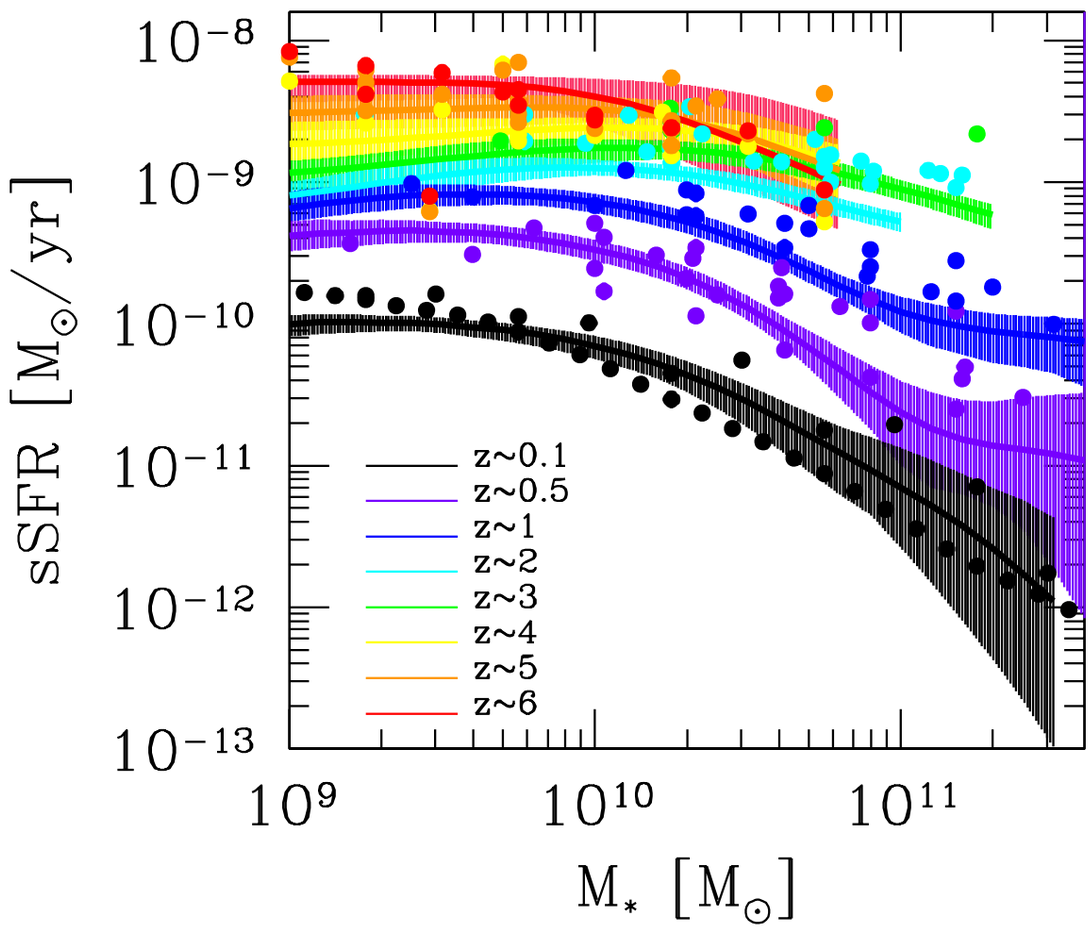

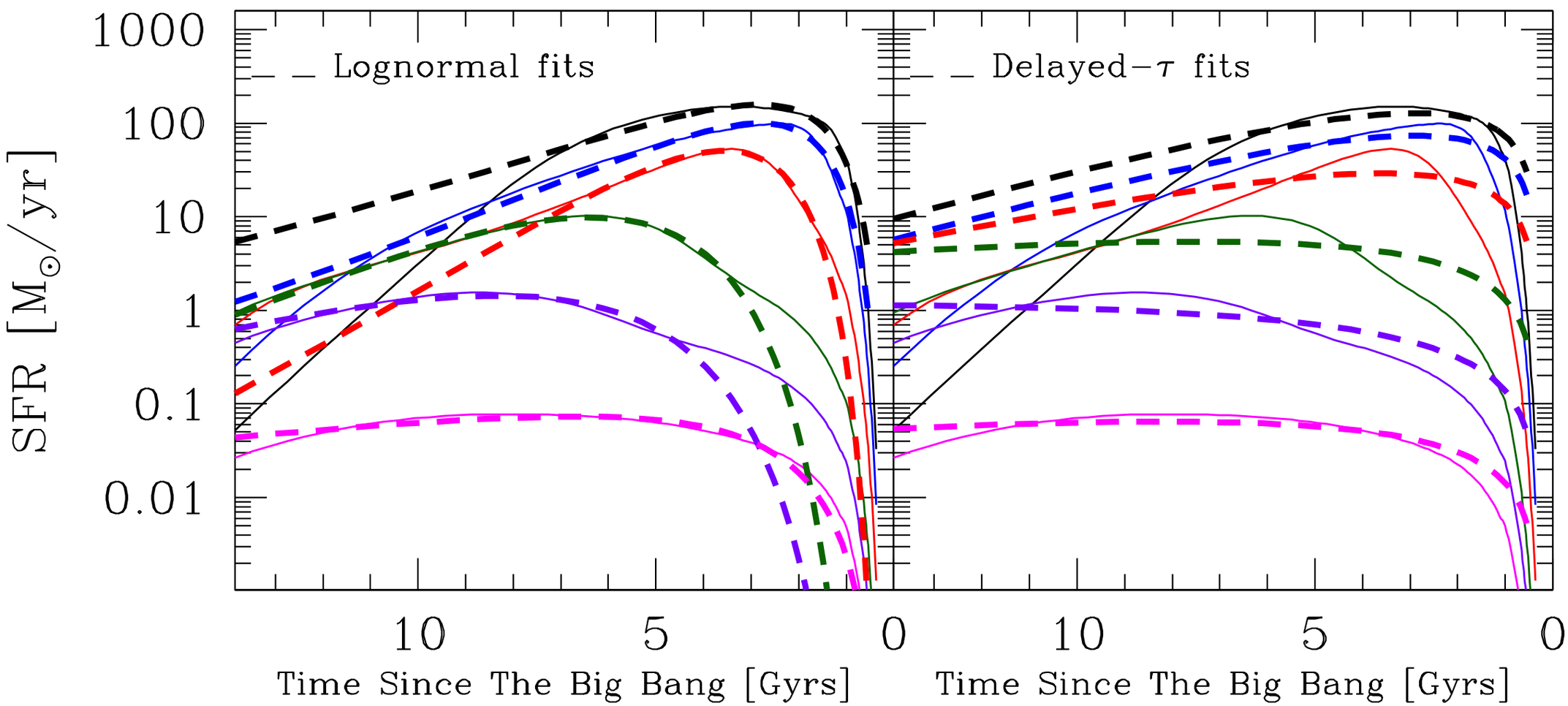

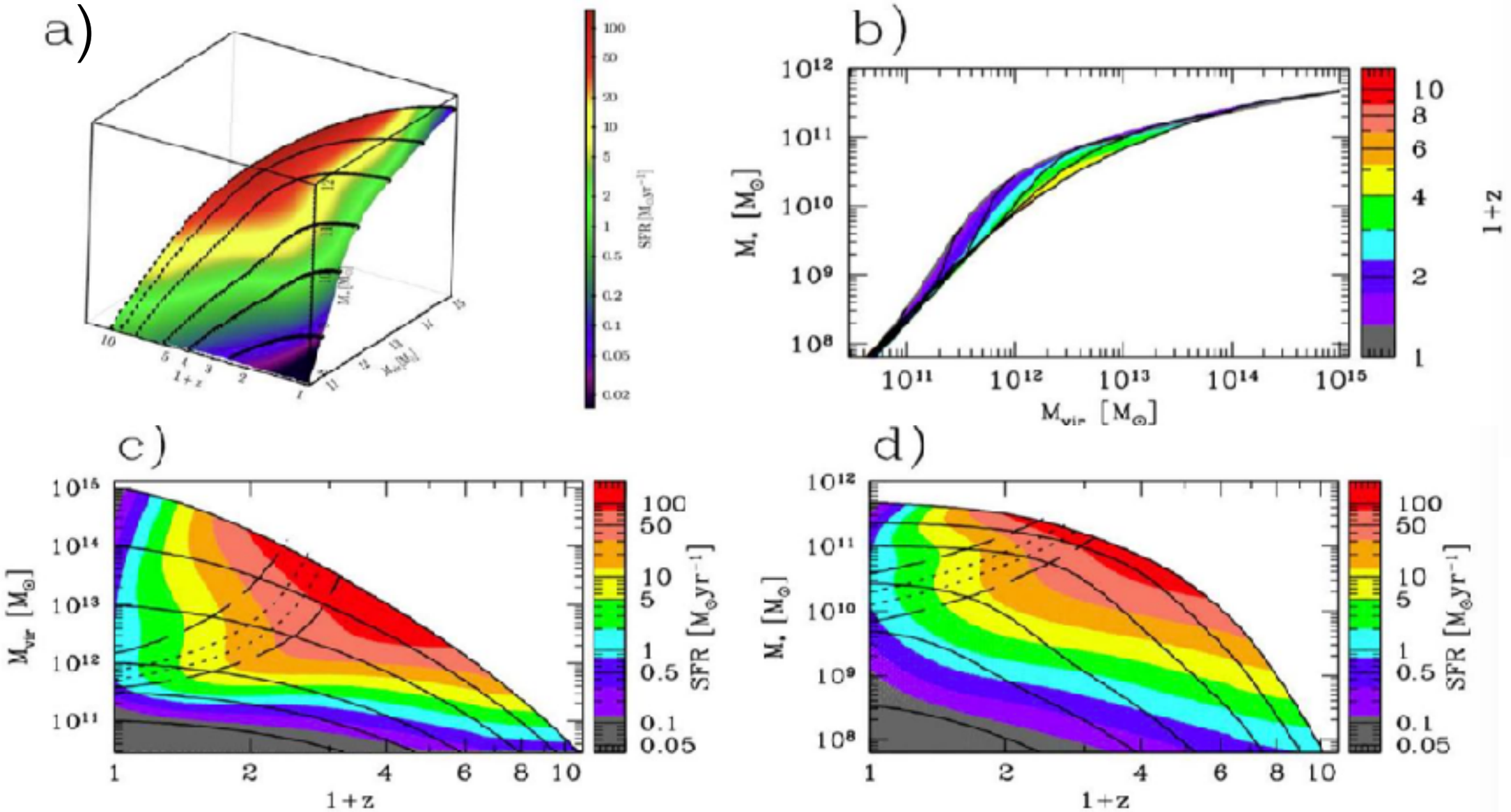

The star formation rate (SFR) as a function of redshift and (left panel) M_{vir} and (right panel) M_*

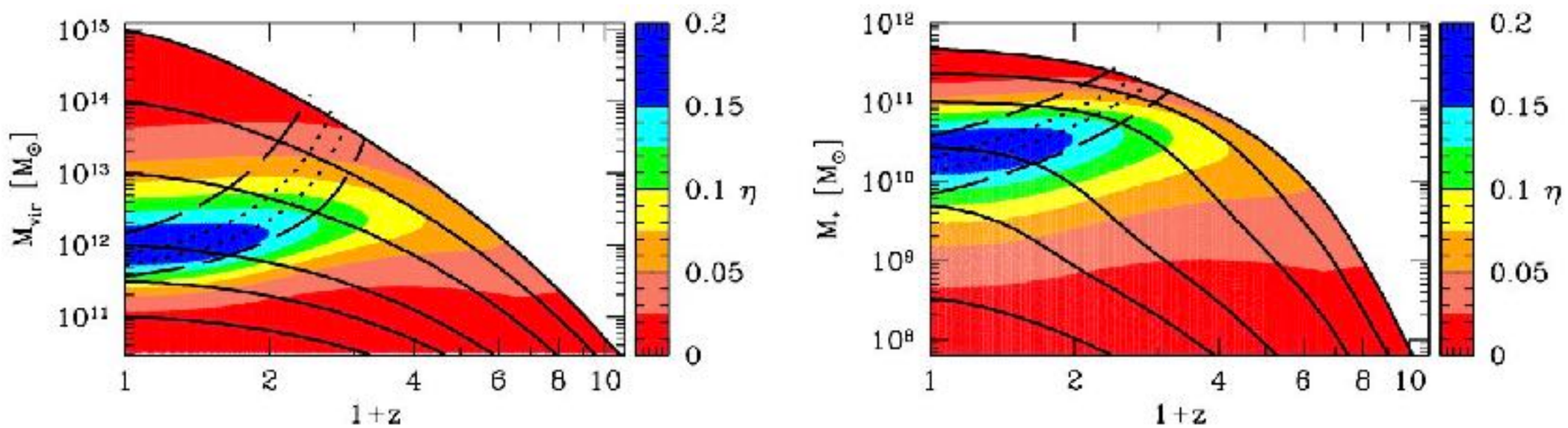

The integral stellar conversion $\eta = f_*/f_b$, where $f_* = M_*/Mvir$ and $f_b = \Omega_B/\Omega_M$

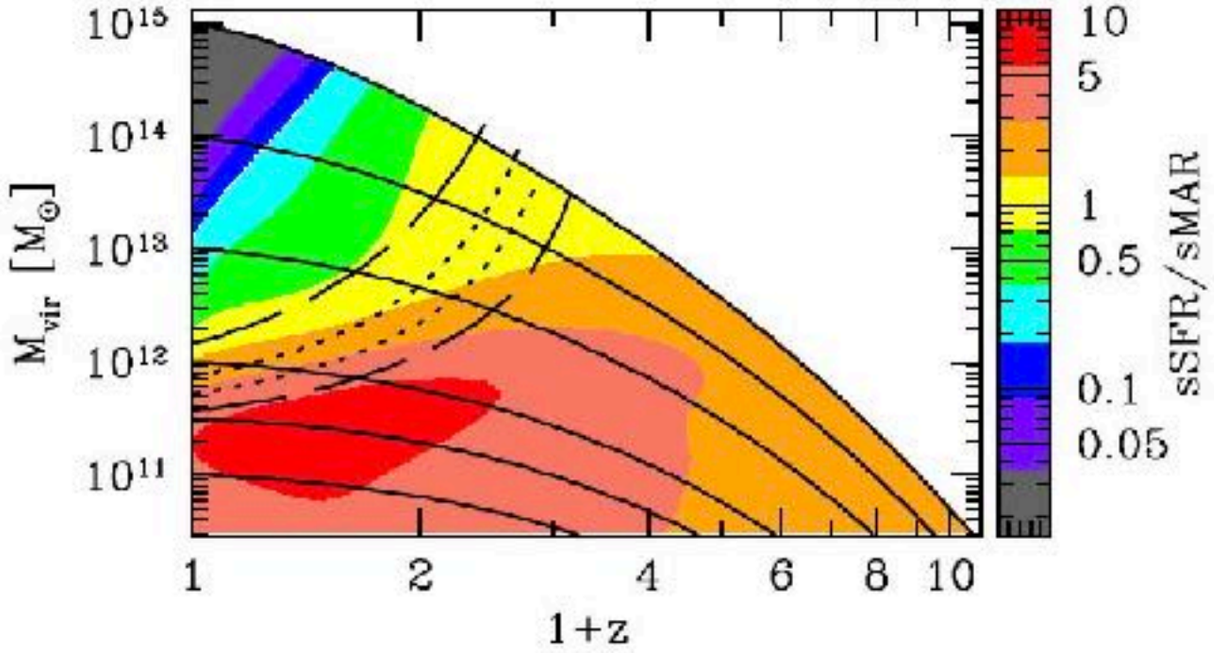

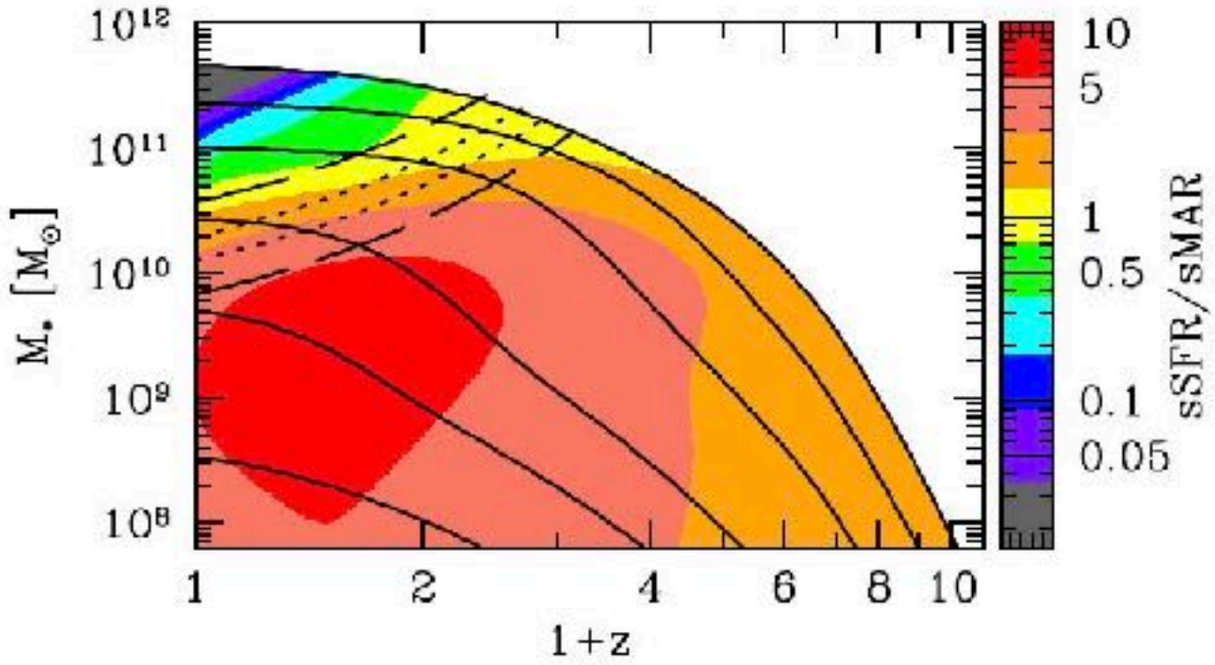

This figure shows that quenching is correlated with sSFR/sSMR = t_{halo}/t_*, since sSFR/sSMR and quenching curves are nearly parallel. sSFR/sSMR
- first rises, reaching a peak ~2 at z ~ 3 for 10^{13} halos, a peak ~7 for 10^{12} halos at z~1.5, and 10^{11} halos are still at peak sSFR/sSMR ~ 10
- then declines along all Mvir and M* progenitor tracks toward z=0.

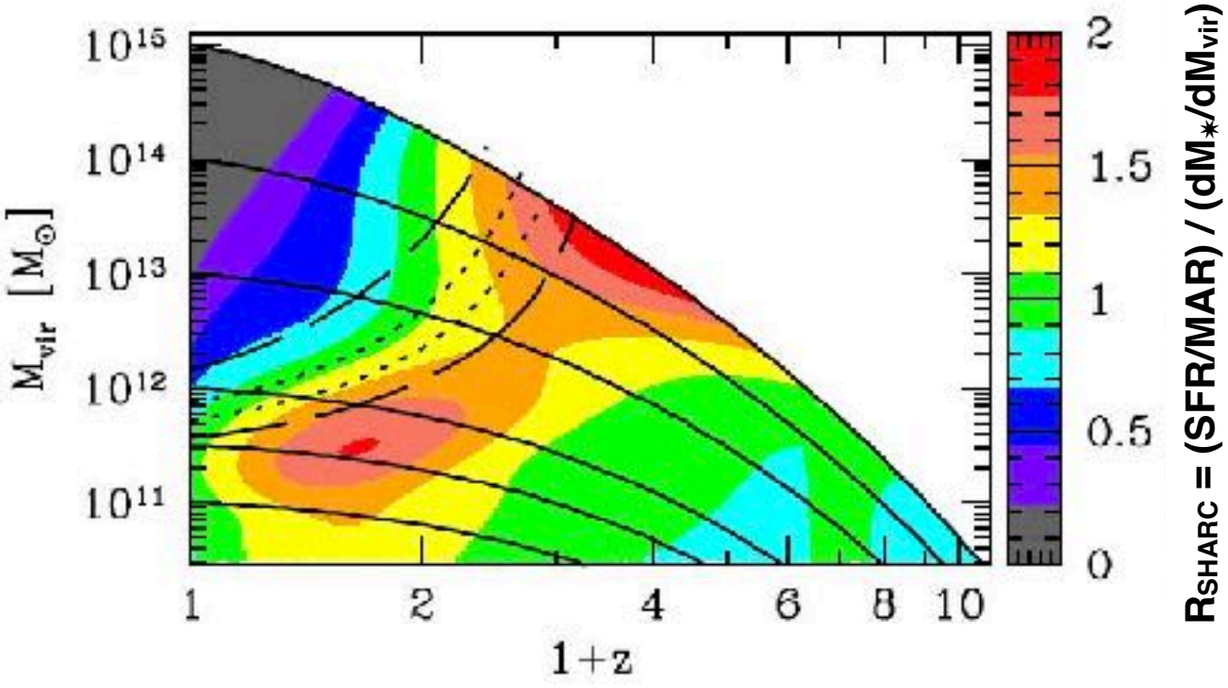

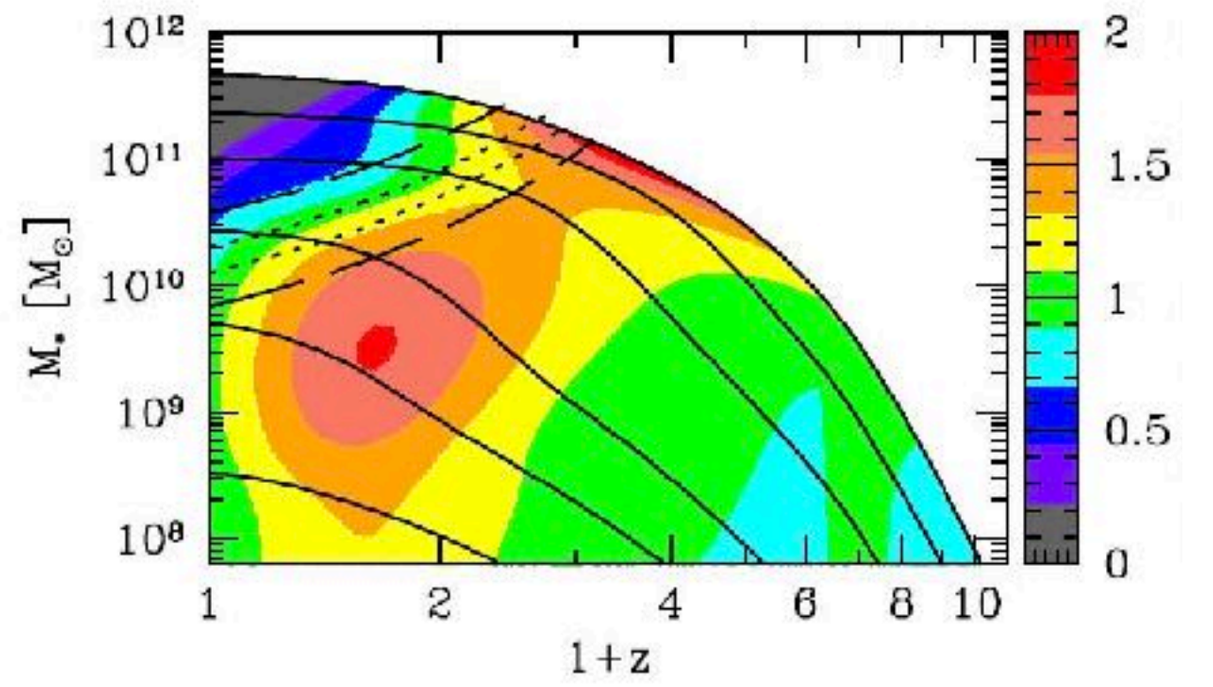

This figure shows that the SHARC approximation is rather well satisfied until quenching, the SHARC ratio R_{SHARC} = (SFR / MAR) / (dM_{vir}/dlog M*) having a value of about 1 to 2 along the progenitor trajectories, and then dropping after quenching. This shows quenching is correlated with R_{SHARC} :

- **the fraction of quenched galaxies is ~ 50% when R_{SHARC} ~ 1 to 1.5, and the quenched fraction is > 75% when R_{SHARC} drops to ~1**
- **like sSFR/sSMR, R_{SHARC} first rises along all progenitor curves, reaches a peak at higher z for higher mass (Mvir or M*), and then declines**
- **unlike sSFR/sSMR, the peak SHARC ratio is nearly constant between 1.5 and 2 (the SHARC ratio peaks at about 2 for both $10^{11.5}$ halos at z ~ 0.5 and 10^{15} halos at z ~ 3, and at about 1.5 for intermediate mass halos).**

Note: the SHARC formula is SFR = (dM_*/dM_{vir}) MAR where MAR = dM_{vir}/dt. Define R_{SHARC} = (SFR / MAR) / (dM_*/dM_{vir}), so SHARC ==> R_{SHARC} = 1.

Constraining the Galaxy Halo Connection: Star Formation Histories, Galaxy Mergers, and Structural Properties, by Aldo Rodriguez-Puebla, Joel, and others (in nearly final form) PREVIEW

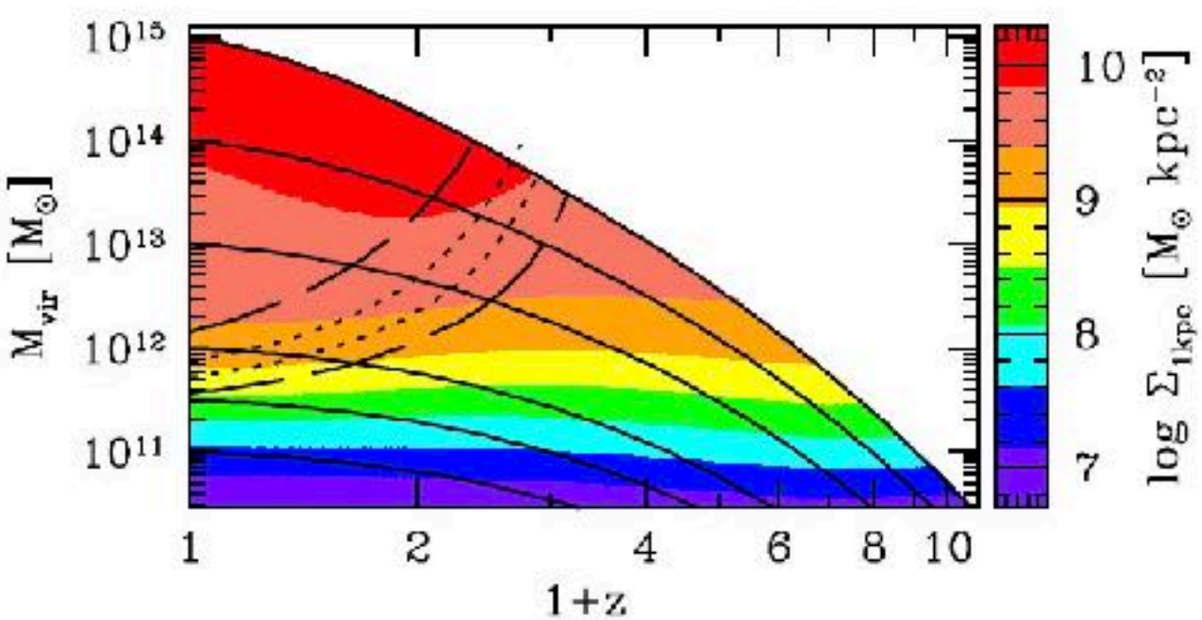

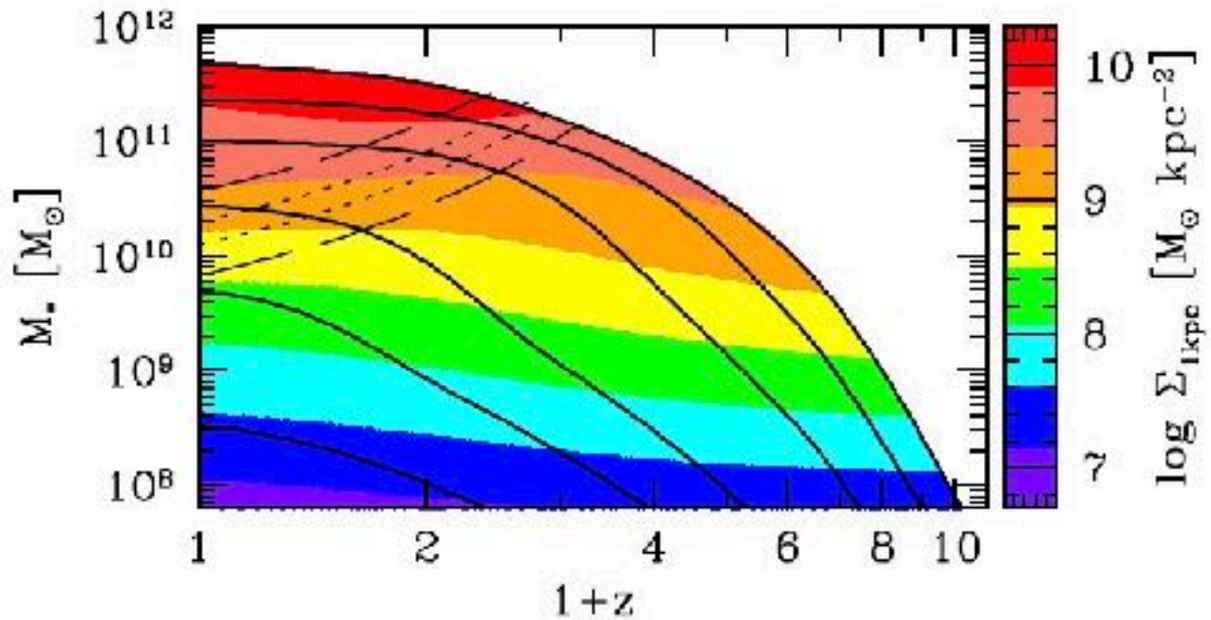

This figure (and the left panel below) shows that Σ_1 reaching a maximum correlates with quenching:
- Σ_1 rises steadily toward z = 0 along all progenitor tracks
- Σ_1 at the quenching transition rises steadily with M_{vir} and reaches its maximum at lower redshifts for lower M_{vir} — "quenching downsizing"
- The fact that the progenitor tracks are parallel to the trajectory curves shows that Σ_1 remains constant after it reaches its maximum

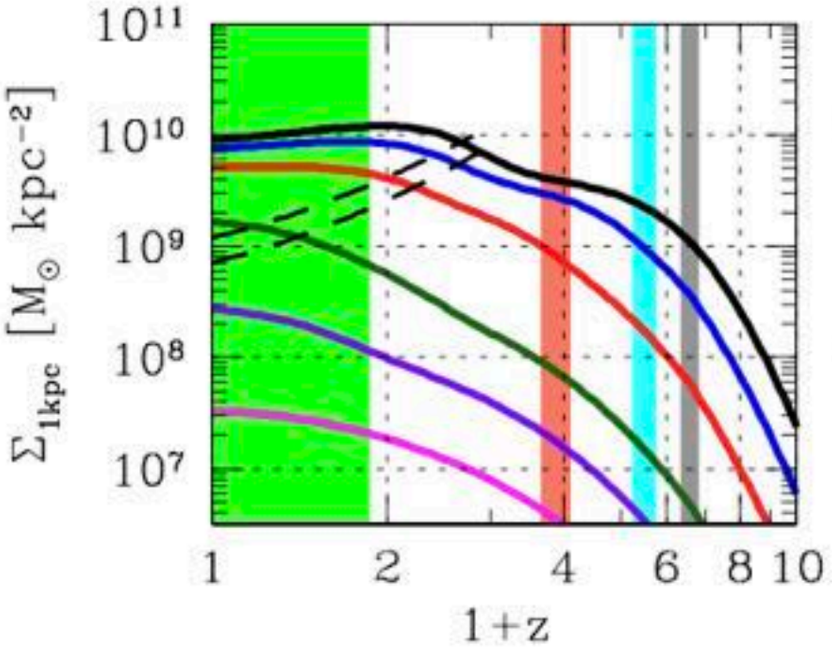

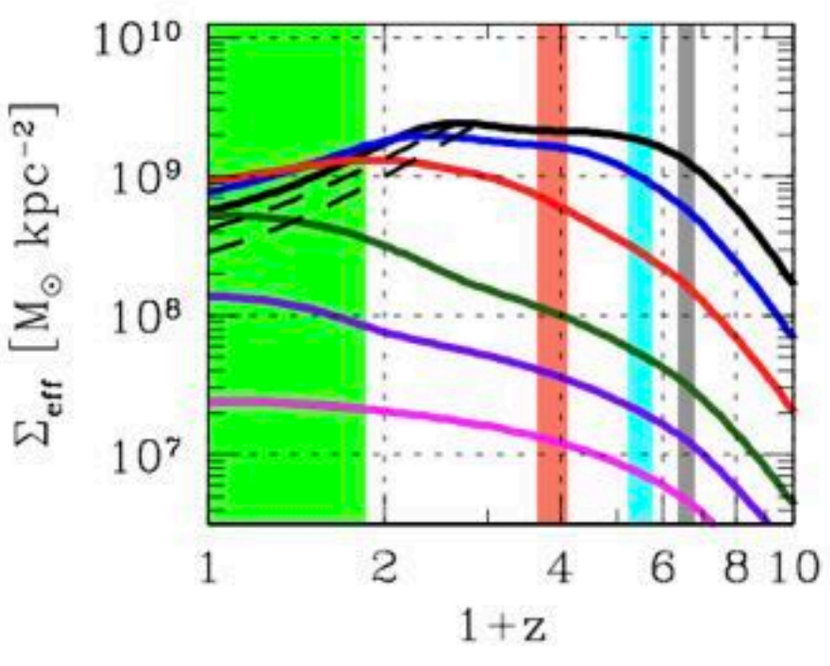

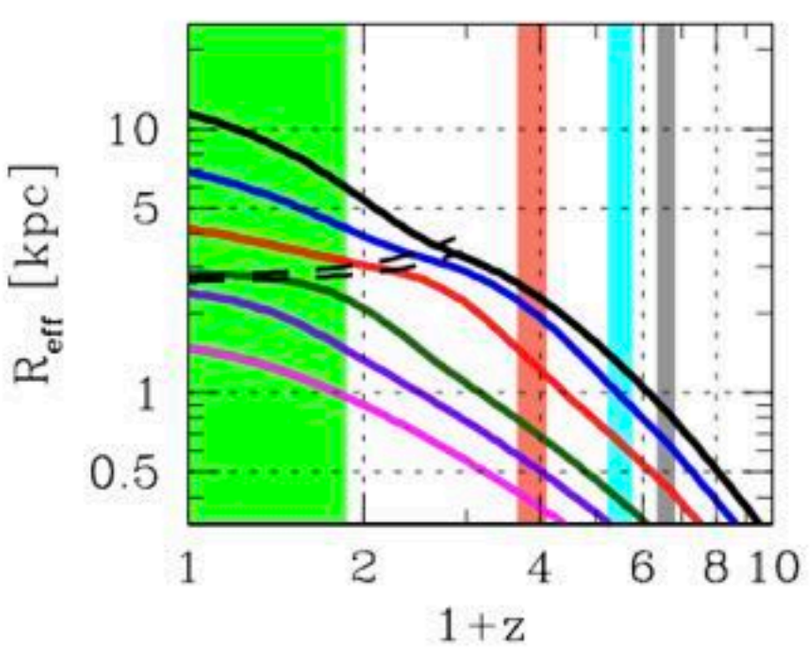

The right panel shows that R_{eff} steadily rises along halo trajectories, and quenching occurs when $R_{eff} \approx 3$ kpc. Although Σ_1 is flat after quenching, the middle panel shows that Σ_{eff} declines after quenching as R_{eff} increases.

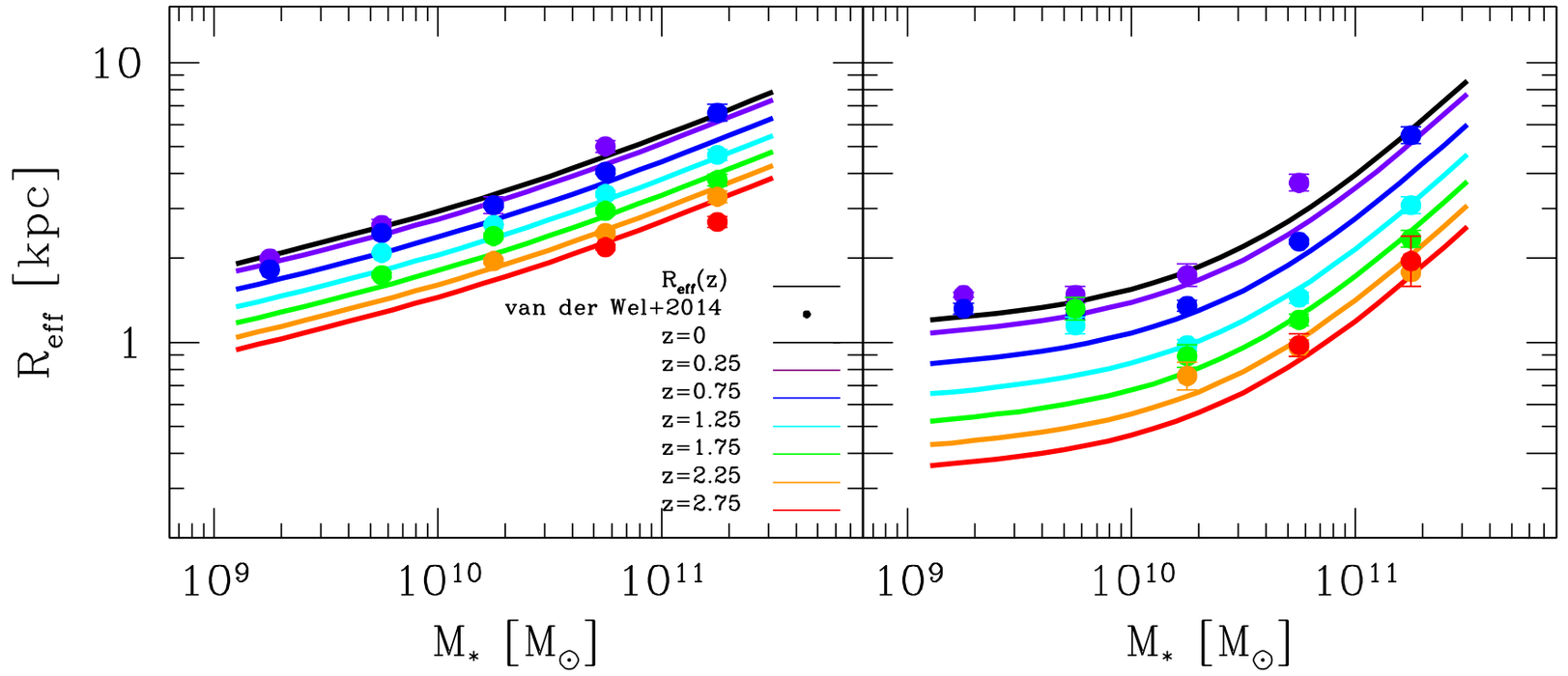

Figure 16. Circularized effective radius for blue star-forming galaxies, left panel, and red quiescent galaxies, right panel. The filled circles show the circularized effective radius as function of redshift from van der Wel et al. (2014) based on multiwavelength photometry from the 3D-HST survey and HST/WFC3 imaging from CANDELS. Solid lines show the redshift dependence for blue and red galaxies of the local relation by Mosleh, Williams & Franx (2013) based on the MPA-JHU SDSS DR7. We utilize the above redshift dependences as an input to derive average galaxy's radial mass distribution as a function of stellar mass by assuming that blue/star-forming galaxies have a Sèrsic index $n = 1$ while red/quenched galaxies have a Sèrsic index $n = 4$ (see text for details).

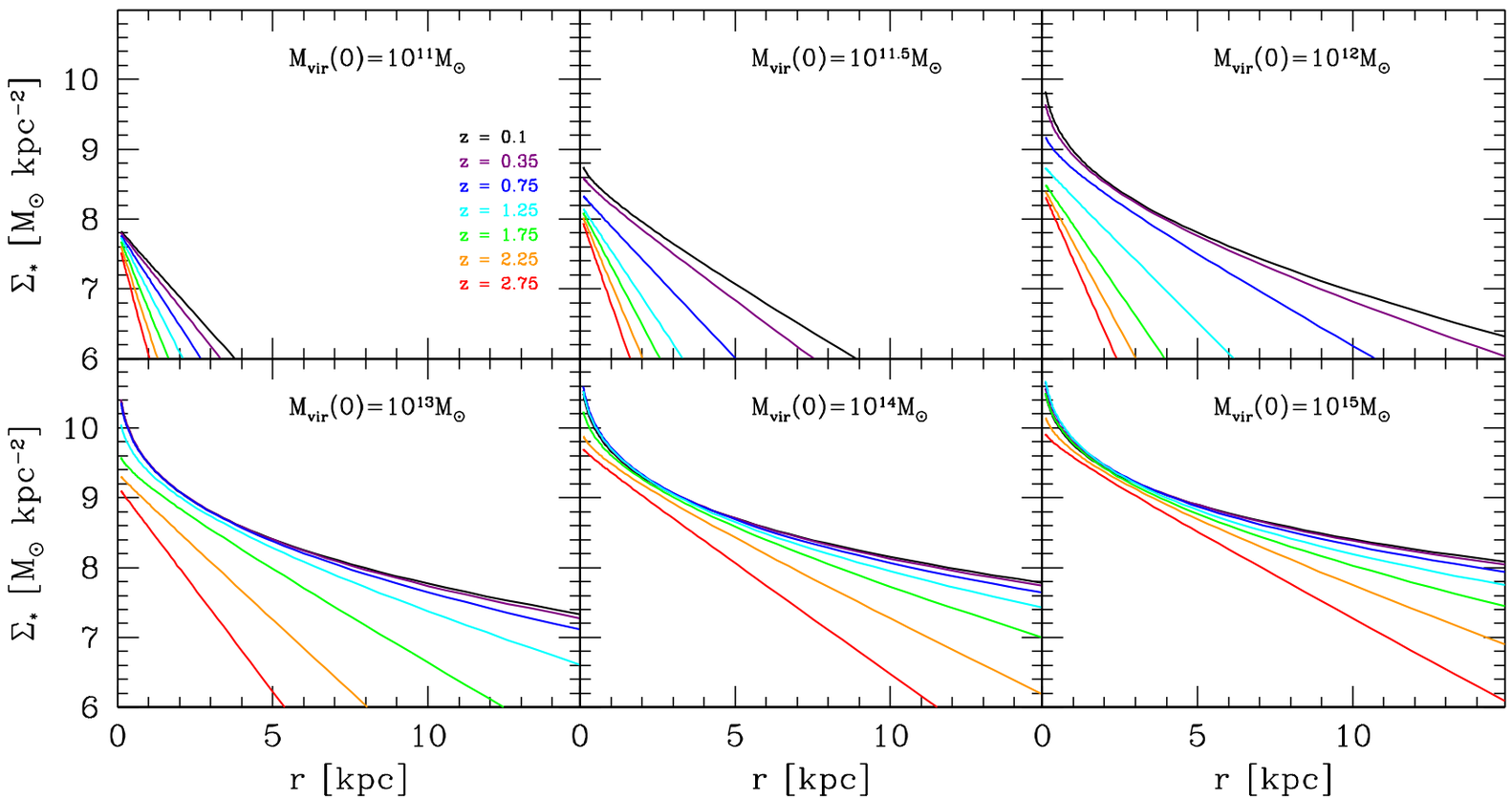

Figure 17. Average evolution of the radial distribution of stellar mass for galaxies in halo progenitors at z = 0 with M_{vir} = 10^{11},$10^{11.5}$,10^{12},10^{13}, 10^{14} and $10^{15}M_\odot$. These radial distributions can be imagined as stacking all the density profiles of galaxies at a given z, no matter whether galaxies are spheroids or disks or a combination of both.

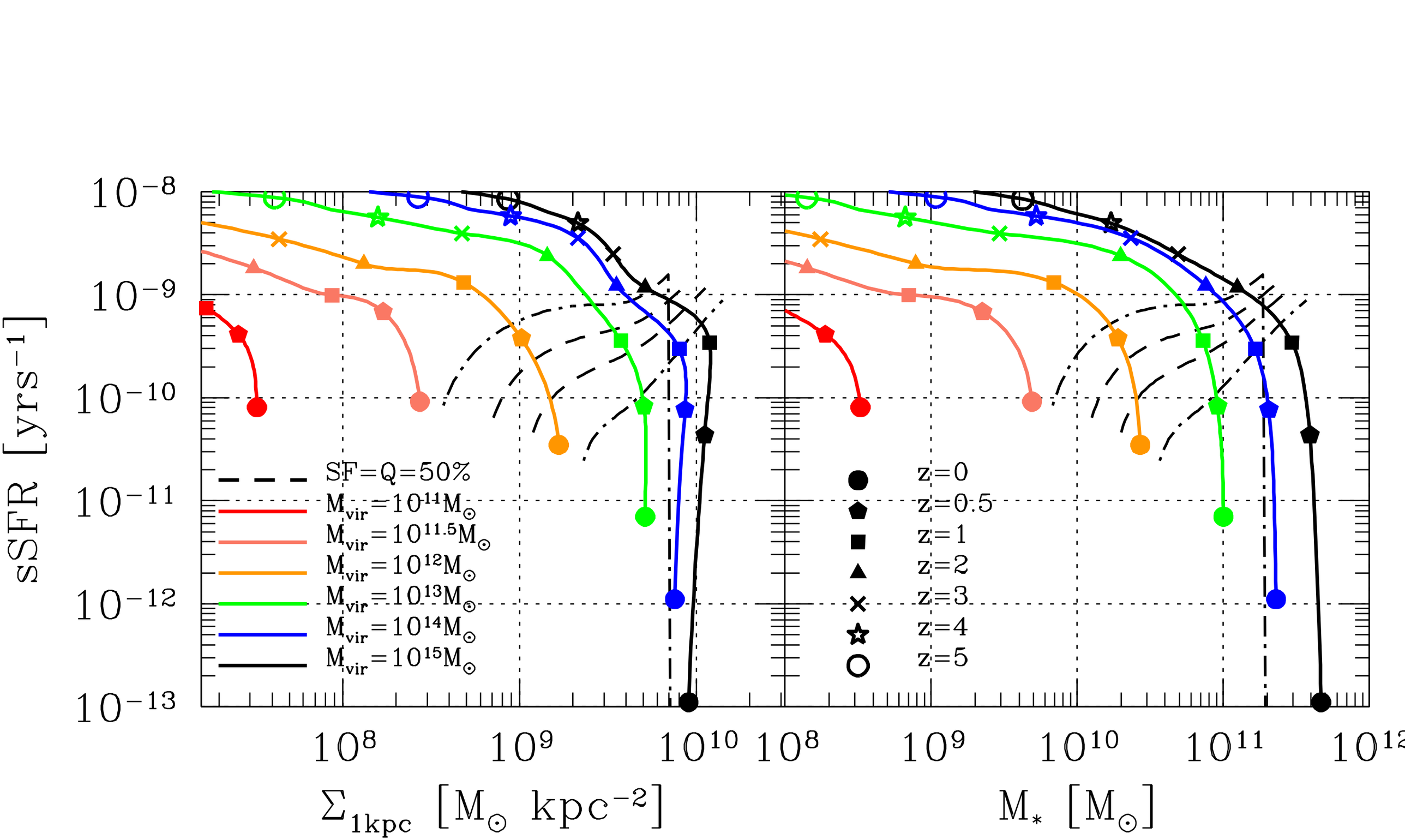
sSFR [yrs^{-1}]
10^{-8}
10^{-9}
10^{-10}
10^{-11}
10^{-12}
10^{-13}
SF=Q=50%
$M_{vir}=10^{11}M_\odot$
$M_{vir}=10^{11.5}M_\odot$
$M_{vir}=10^{12}M_\odot$
$M_{vir}=10^{13}M_\odot$
$M_{vir}=10^{14}M_\odot$
$M_{vir}=10^{15}M_\odot$
z=0
z=0.5
z=1
z=2
z=3
z=4
z=5
10^8
10^9
10^{10}
10^{11}
10^{12}
Σ_{1kpc} [$M_\odot$ kpc^{-2}]
M_* [$M_\odot$]

Change in slope in Reff - M* diagram after quenching

SF=Q=50%
$M_{vir}=10^{11}M_\odot$
$M_{vir}=10^{11.5}M_\odot$
$M_{vir}=10^{12}M_\odot$
$M_{vir}=10^{13}M_\odot$
$M_{vir}=10^{14}M_\odot$
$M_{vir}=10^{15}M_\odot$

z=0
z=0.5
z=1
z=2
z=3
z=4
z=5

R_{eff} [kpc]

10
5
1
0.5

Minor Mergers

Major Mergers

$\mathcal{R}_m$ [Gyr^{-1}]

10
1
0.1
0.01

10^8 10^9 10^{10} 10^{11}

M_* [$M_\odot$]

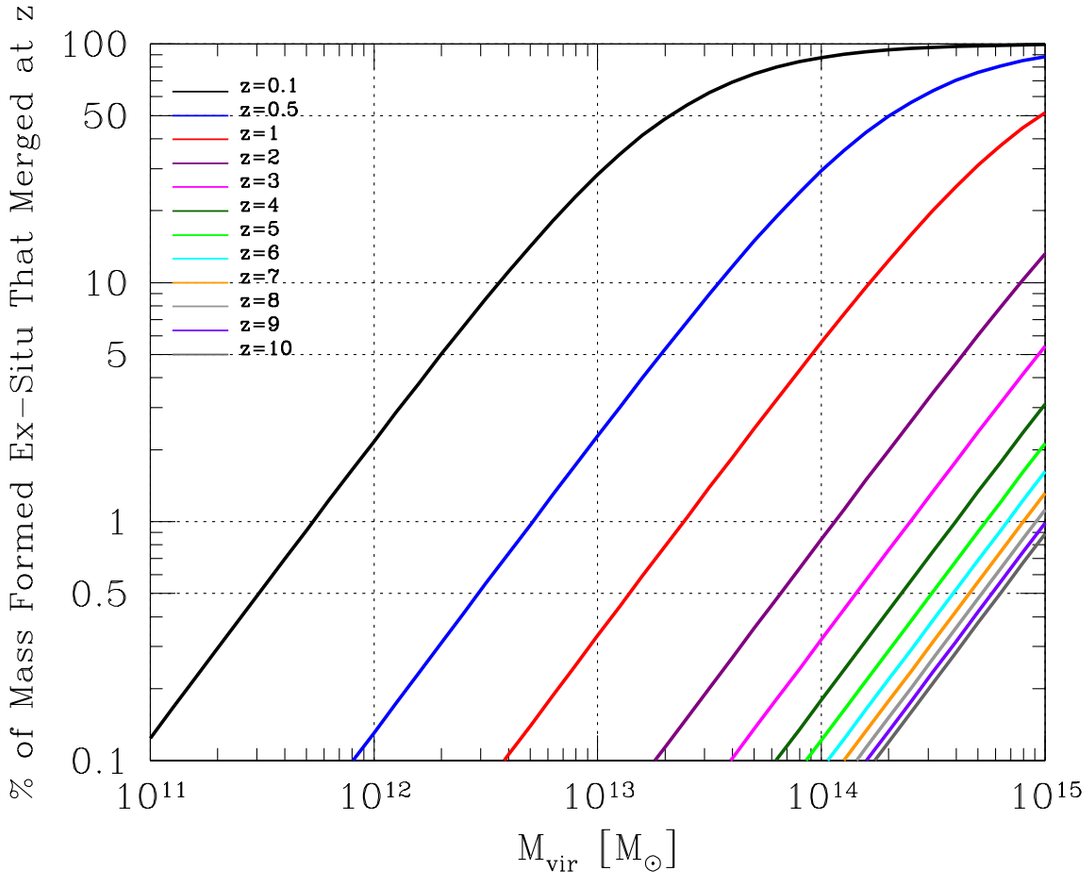

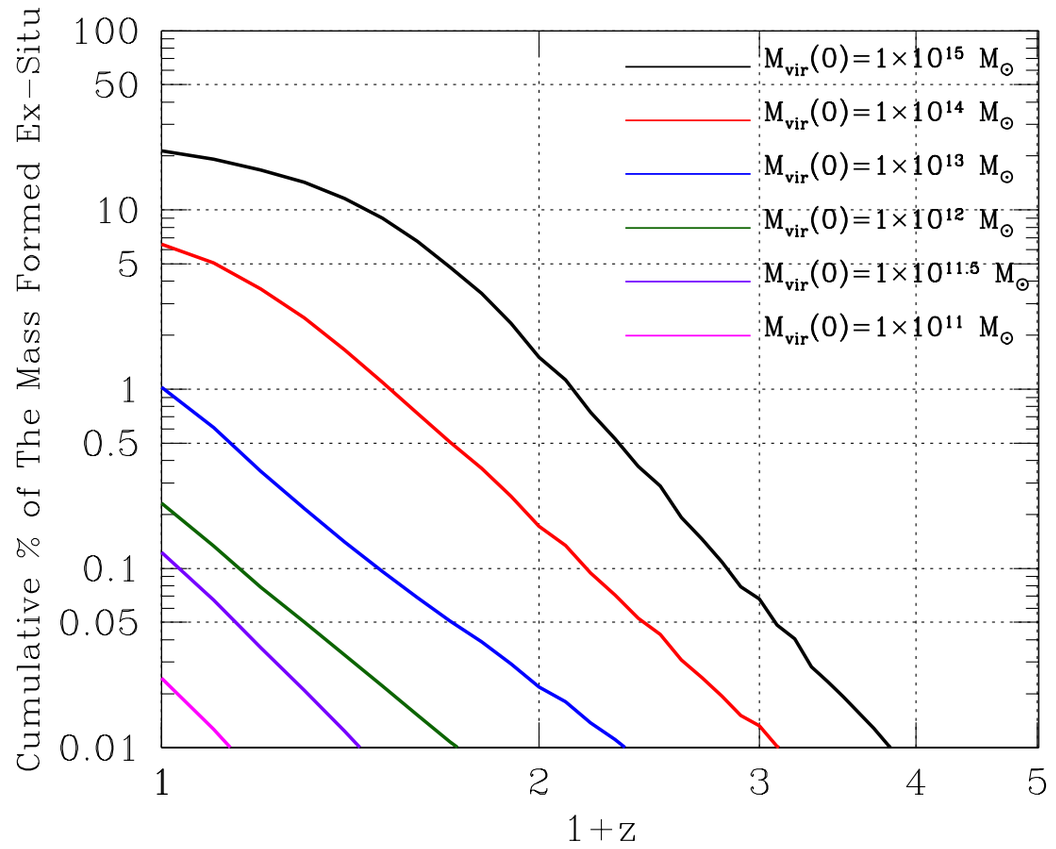

Figure 13. Left Panel: Instantaneous fraction of mass that formed ex-situ and was accreted by galaxy mergers as a function of the halo mass at redshift $z = 0$. **Right Panel:** Cumulative fraction of mass that formed ex-situ and accreted through galaxy mergers. Note that 20% of the final mass in host galaxies of halos with $M_{\rm vir}(0) = 1 \times 10^{15}$ was accreted by galaxy mergers.

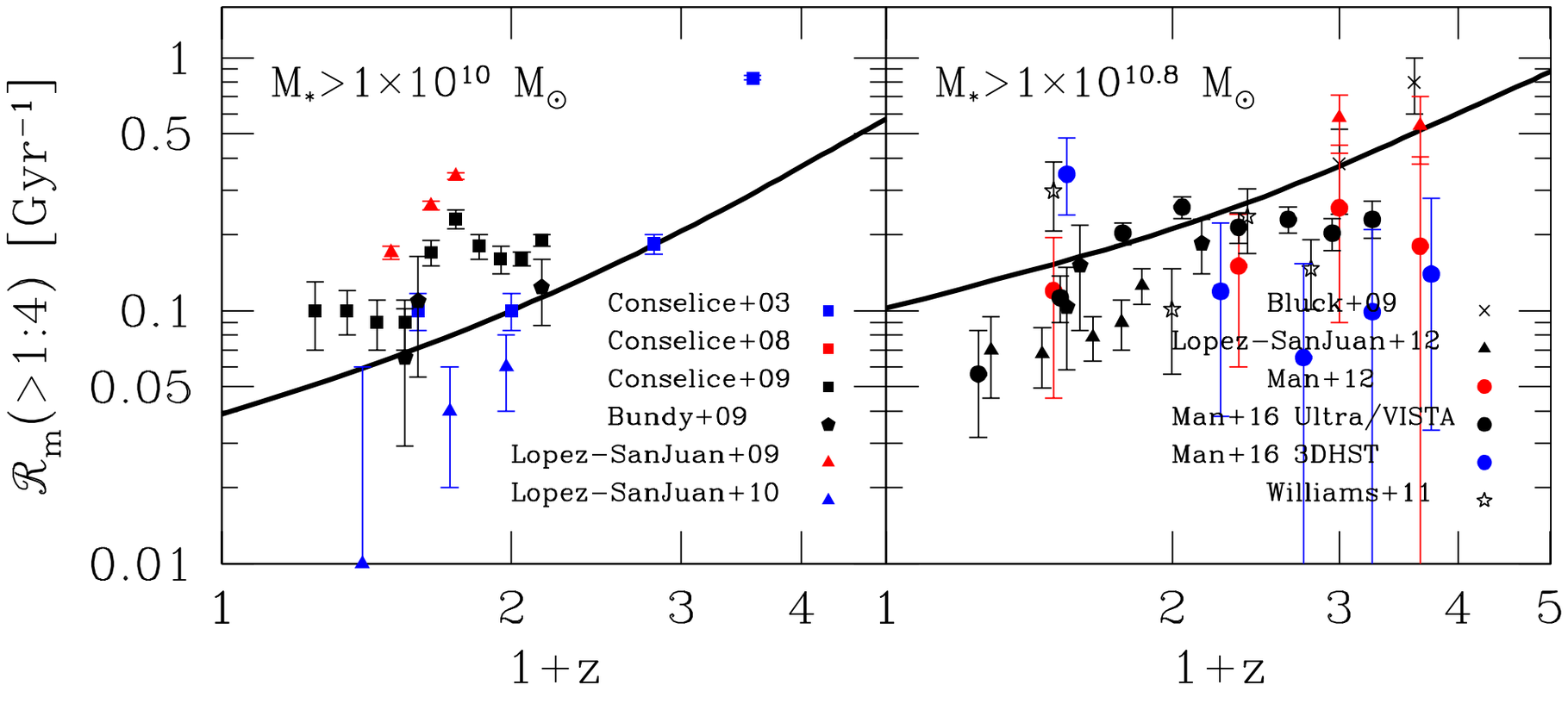

Figure 14. Left Panel: Galaxy major merger rate for galaxies with masses above $1 \times 10^{10} M_*$. Solid lines show the predictions based on our new SHMR while the different symbols show observational estimates from Conselice et al. (2003); Conselice, Rajgor & Myers (2008); Conselice, Yang & Bluck (2009); L´opez-Sanjuan et al. (2009) and L´opez-Sanjuan et al. (2010) based on galaxy asymmetries while Bundy et al. (2009) gives the merger rate fraction from galaxy pairs. Right Panel: Similarly above but for galaxies with masses above $1{\times}10^{10.8} M_*$. Symbols are fromBluck et al. (2009) using galaxy asymmetries, L´opez-Sanjuan et al. (2012); Man et al. (2012); Man, Zirm & Toft (2016) and Williams, Quadri & Franx (2011) based on galaxy pairs.